A&A 520, A28 (2010)
DOI: 10.1051/0004-6361/201014700

Astronomy & Astrophysics

Test-field method for mean-field coefficients with MHD background

M. Rheinhardt[1] and A. Brandenburg[1,2]

[1] NORDITA, AlbaNova University Center, Roslagstullsbacken 23, 10691 Stockholm, Sweden
e-mail: mreinhardt@aip.de
[2] Department of Astronomy, AlbaNova University Center, Stockholm University, 10691 Stockholm, Sweden

Received 1 April 2010 / Accepted 27 May 2010

ABSTRACT

Aims. The test-field method for computing turbulent transport coefficients from simulations of hydromagnetic flows is extended to the regime with a magnetohydrodynamic (MHD) background.

Methods. A generalized set of test equations is derived using both the induction equation and a modified momentum equation. By employing an additional set of auxiliary equations, we obtain linear equations describing the response of the system to a set of prescribed test fields. Purely magnetic and MHD backgrounds are emulated by applying an electromotive force in the induction equation analogously to the ponderomotive force in the momentum equation. Both forces are chosen to have Roberts-flow like geometry.

Results. Examples with purely magnetic as well as MHD backgrounds are studied where the previously used quasi-kinematic test-field method breaks down. In cases with homogeneous mean fields it is shown that the generalized test-field method produces the same results as the imposed-field method, where the field-aligned component of the actual electromotive force from the simulation is used. Furthermore, results for the turbulent diffusivity are given, which are inaccessible to the imposed-field method. For MHD backgrounds, new mean-field effects are found that depend on the occurrence of cross-correlations between magnetic and velocity fluctuations. In particular, there is a contribution to the mean Lorentz force that is linear in the mean field and hence reverses sign upon a reversal of the mean field. For strong mean fields, α is found to be quenched proportional to the fourth power of the field strength, regardless of the type of background studied.

Key words. magnetohydrodynamics – dynamo – Sun: dynamo – stars: magnetic field – methods: numerical

1. Introduction

Astrophysical bodies such as stars with outer convective envelopes, accretion discs, and galaxies tend to be magnetized. In all those cases the magnetic field varies on a broad spectrum of scales. On small scales the magnetic field might well be the result of scrambling an existing large-scale field by a small-scale flow. However, at large magnetic Reynolds numbers, i.e. when advection dominates over magnetic diffusion, another source of small-scale fields is small-scale dynamo action (Kazantsev 1968). This process is now fairly well understood and confirmed by numerous simulations (Cho & Vishniac 2000; Schekochihin et al. 2002, 2004; Haugen et al. 2003, 2004); for a review see Brandenburg & Subramanian (2005). Especially in the context of magnetic fields of galaxies, the occurrence of small-scale dynamos may be important for providing a strong field on short time scales (10^7 yr), which may then act as the seed for a large-scale dynamo (Beck et al. 1994).

In contemporary galaxies the strength of magnetic fields on small and large length scales is comparable (Beck et al. 1996), but in stars this is less clear. On the solar surface the solar magnetic field shows significant energy in small scales. (Solanki et al. 2006). The possibility of generating such magnetic fields locally in the upper layers of the convection zone by a small-scale dynamo is sometimes referred to as *surface dynamo* (Cattaneo 1999; Emonet & Cattaneo 2001; Vögler & Schüssler 2007). On the other hand, simulations of stratified convection with shear show that small-scale dynamo action is a prevalent feature of the kinematic regime, but becomes less important when the field is strong and saturated (Brandenburg 2005a; Käpylä et al. 2008).

An important question is then how the primary presence of small-scale magnetic fields affects the generation of large-scale fields if these are the result of a large-scale dynamo. Such a process creates magnetic fields on scales large compared with those of the energy-carrying eddies of the underlying, in general turbulent flow via an instability (Parker 1979). A commonly used tool for studying this type of dynamos is mean-field electrodynamics, where correlations of small-scale magnetic and velocity fields are expressed in terms of the mean magnetic field and the mean velocity using corresponding turbulent transport coefficients or their associated integral kernels (Moffatt 1978; Krause & Rädler 1980). The determination of these coefficients (e.g., α effect and turbulent diffusivity) is the central task of mean-field dynamo theory. This can be performed analytically, but usually only via approximations which are hardly justified in realistic astrophysical situations where the magnetic Reynolds numbers, $\mathrm{Re_M}$, are large.

Obtaining turbulent transport coefficients from direct numerical simulations (DNS) offers a more sustainable alternative as it avoids the restricting approximations and uncertainties of analytic approaches. Moreover, no assumptions concerning correlation properties of the turbulence need to be made, because a direct "measurement" of those properties is performed in a physically consistent situation emulated by the DNS. The simplest way to accomplish such a measurement is to include an imposed large-scale magnetic field in the DNS, whose influence on the fluctuations of magnetic field and velocity is utilized in inferring a subset of the relevant transport coefficients. We refer to this technique as the *imposed-field method*. As an important limitation, it has to be required that the actual mean field in the main run, which may differ from the initially imposed one, is uniform. Otherwise the results will be corrupted (Käpylä et al. 2010).

A more universal tool is offered by the *test-field method* (Schrinner et al. 2005, 2007), which allows the determination of all wanted transport coefficients from a single DNS. For this purpose the fluctuating velocity is taken from the DNS and inserted into a properly tailored set of *test equations*. Their solutions, the *test solutions*, represent fluctuating magnetic fields as responses to the interaction of the fluctuating velocity with a set of suitably chosen mean fields, the *test fields*. For distinction from the test equations, which are in general also solved by direct numerical simulation, we will refer to the original DNS as the *main run*. This method has been successfully applied to homogeneous turbulence with helicity (Sur et al. 2008; Brandenburg et al. 2008a), with shear and no helicity (Brandenburg et al. 2008b), and with both (Mitra et al. 2009).

A crucial requirement on any test-field method is the independence of the resulting transport coefficients on the strength and geometry of the test fields. This is immediately plausible in the kinematic situation, i.e., if there is no back-reaction of the mean magnetic field on the flow. Indeed, for given magnetic boundary conditions and a given value of the magnetic diffusivity, the transport coefficients must not reflect anything else than correlation properties of the velocity field which are completely determined by the hydrodynamics alone. For this to be guaranteed the test equations have to be linear and the test solutions have to be linear and homogeneous in the test fields.

Beyond the kinematic situation the same requirement still holds, although the flow is now modified by a mean magnetic field occurring in the main run. (Whether it is maintained by external sources or generated by a dynamo process does not matter in this context.) Consequently, the transport coefficients are now functionals of this mean field. It is no longer so obvious that under these circumstances a test-field method with the aforementioned linearity and homogeneity properties can be established at all. Nevertheless, it turned out that the method developed for the kinematic situation gives consistent results even in the nonlinear case without any modification (Brandenburg et al. 2008c). This method, which we will refer to as "quasi-kinematic" is, however, restricted to situations in which the magnetic fluctuations are solely a consequence of the mean magnetic field. (That is, the primary or background turbulence is purely hydrodynamic.)

The power of the quasi-kinematic method was demonstrated based on simulations of an α^2 dynamo where the main run had reached saturation with mean magnetic fields of the Beltrami type (Brandenburg et al. 2008c). Magnetic and fluid Reynolds numbers up to 600 were taken into account, so in some of the high Re_M runs there was certainly small-scale dynamo action, that is, a primary magnetic turbulence $\boldsymbol{b}_0$ had to be expected. Nevertheless, the quasi-kinematic method was found to work reliably even for strongly saturated dynamo fields. This was revealed by verifying that the analytically solvable mean-field dynamo model employing the values of α and turbulent diffusivity as derived from the saturated state of the main run indeed yielded a vanishing growth rate. A coexisting small-scale dynamo had very likely saturated at a low level and could thus not create a marked error.

Indeed, the purpose of our work is to propose a generalized test-field method that allows for the presence of magnetic fluctuations in the background turbulence. Moreover, its validity range should cover dynamically effective mean fields, that is, situations in which velocity and magnetic field fluctuations are significantly affected by the mean field.

With a view to this generalization we will first recall the mathematical justification of the quasi-kinematic method and indicate the reason for its limited applicability (Sect. 2). In Sect. 3 the foundation of the generalized method will be laid down in the context of a set of simplified model equations. In Sect. 4 results will be presented for various combinations of hydrodynamic and magnetic backgrounds having Roberts-flow geometry. The astrophysical relevance of our results and their connection to a paper by Courvoisier et al. (2010) who already pointed out the limitation of the quasi-kinematic method will be discussed in Sect. 5.

2. Justification of the quasi-kinematic test-field method and its limitation

In the following we split any relevant physical quantity F into mean and fluctuating parts, $\overline{F}$ and f. No specific averaging procedure will be adopted at this point; we merely assume the Reynolds rules to be obeyed. Furthermore, we split the fluctuations of magnetic field and velocity, $\boldsymbol{b}$ and $\boldsymbol{u}$, into parts existing already in the absence of a mean magnetic field, $\boldsymbol{b}_0$ and $\boldsymbol{u}_0$ (together they form the *background turbulence*), and parts vanishing with $\overline{\boldsymbol{B}}$, denoted by $\boldsymbol{b}_{\overline{B}}$ and $\boldsymbol{u}_{\overline{B}}$. We may split the mean electromotive force $\overline{\boldsymbol{\mathcal{E}}} = \overline{\boldsymbol{u}\times\boldsymbol{b}}$ likewise and get

$$\overline{\boldsymbol{\mathcal{E}}} = \overline{\boldsymbol{\mathcal{E}}}_0 + \overline{\boldsymbol{\mathcal{E}}}_{\overline{B}} \tag{1}$$

with

$$\overline{\boldsymbol{\mathcal{E}}}_0 = \overline{\boldsymbol{u}_0\times\boldsymbol{b}_0}, \qquad \overline{\boldsymbol{\mathcal{E}}}_{\overline{B}} = \overline{\boldsymbol{u}_0\times\boldsymbol{b}_{\overline{B}}} + \overline{\boldsymbol{u}_{\overline{B}}\times\boldsymbol{b}_0} + \overline{\boldsymbol{u}_{\overline{B}}\times\boldsymbol{b}_{\overline{B}}}. \tag{2}$$

Note that we do not restrict $\boldsymbol{b}_{\overline{B}}$ and $\boldsymbol{u}_{\overline{B}}$, and therefore also not $\overline{\boldsymbol{\mathcal{E}}}_{\overline{B}}$, to a certain order in $\overline{\boldsymbol{B}}$.

In the present section we assume that the background turbulence is purely hydrodynamic, that is, $\boldsymbol{b}_0 = \boldsymbol{0}$ and hence $\boldsymbol{b} = \boldsymbol{b}_{\overline{B}}$. This is possible if there is neither an external electromotive force in the induction equation nor a small-scale dynamo. Thus, the magnetic fluctuations $\boldsymbol{b}$ are entirely a consequence of the interaction of the velocity fluctuations $\boldsymbol{u}$ with the mean field $\overline{\boldsymbol{B}}$.

In a homogeneous medium, the induction equations for the total, mean and fluctuating magnetic fields read

$$\frac{\partial \boldsymbol{B}}{\partial t} = \eta\nabla^2\boldsymbol{B} + \mathrm{curl}\,(\boldsymbol{U}\times\boldsymbol{B}), \tag{3}$$

$$\frac{\partial \overline{\boldsymbol{B}}}{\partial t} = \eta\nabla^2\overline{\boldsymbol{B}} + \mathrm{curl}\,(\overline{\boldsymbol{U}}\times\overline{\boldsymbol{B}} + \overline{\boldsymbol{\mathcal{E}}}), \tag{4}$$

$$\frac{\partial \boldsymbol{b}}{\partial t} = \eta\nabla^2\boldsymbol{b} + \mathrm{curl}\,(\overline{\boldsymbol{U}}\times\boldsymbol{b} + \boldsymbol{u}\times\overline{\boldsymbol{B}} + \boldsymbol{\mathcal{E}}'), \tag{5}$$

with $\boldsymbol{\mathcal{E}}' = \boldsymbol{u}\times\boldsymbol{b} - \overline{\boldsymbol{u}\times\boldsymbol{b}}$. The solution of the linear Eq. (5) for the fluctuations $\boldsymbol{b}$, *considered as a functional of* $\boldsymbol{u}$, $\overline{\boldsymbol{U}}$ *and* $\overline{\boldsymbol{B}}$, is linear and homogeneous in the latter and the same is true for

$$\overline{\boldsymbol{\mathcal{E}}}_{\overline{B}} = \overline{\boldsymbol{\mathcal{E}}} = \overline{\boldsymbol{u}\times\boldsymbol{b}_{\overline{B}}} = \overline{\boldsymbol{u}\times\boldsymbol{b}}. \tag{6}$$

If the velocity is influenced by the mean field, that is, if $\boldsymbol{u}$ and $\overline{\boldsymbol{U}}$ depend on $\overline{\boldsymbol{B}}$, $\overline{\boldsymbol{\mathcal{E}}}$ considered as a functional of $\overline{\boldsymbol{B}}$, $\overline{\boldsymbol{\mathcal{E}}}\{\overline{\boldsymbol{B}}\}$, is of course nonlinear. However, $\overline{\boldsymbol{\mathcal{E}}}$, again considered as a functional of $\boldsymbol{u}$, $\overline{\boldsymbol{U}}$ and $\overline{\boldsymbol{B}}$, $\overline{\boldsymbol{\mathcal{E}}}\{\boldsymbol{u}, \overline{\boldsymbol{U}}, \overline{\boldsymbol{B}}\}$, is still linear in $\overline{\boldsymbol{B}}$.

The major task of mean-field theory consists now just in establishing the linear and homogeneous functional relating $\overline{\boldsymbol{\mathcal{E}}}$ to $\overline{\boldsymbol{B}}$. Making the ansatz

$$\overline{\boldsymbol{\mathcal{E}}} = \boldsymbol{\alpha}\overline{\boldsymbol{B}} - \boldsymbol{\eta}\boldsymbol{\nabla}\overline{\boldsymbol{B}}, \tag{7}$$

with $\boldsymbol{\nabla}\overline{\boldsymbol{B}}$ being the gradient tensor of the mean magnetic field, this task coincides with determining the tensors $\boldsymbol{\alpha}$ and $\boldsymbol{\eta}$, which are of course functionals of $\boldsymbol{u}$ and $\overline{\boldsymbol{U}}$. Because of linearity and homogeneity we are entitled to employ for this purpose various *arbitrary* vector fields $\overline{\boldsymbol{B}}^{\mathrm{T}}$ (the *test fields*) in place of $\overline{\boldsymbol{B}}$ in Eq. (5), keeping the velocity of course fixed. Each specific assignment of $\overline{\boldsymbol{B}}^{\mathrm{T}}$ yields a corresponding $\boldsymbol{b}^{\mathrm{T}}$ and via that an $\overline{\boldsymbol{\mathcal{E}}}^{\mathrm{T}}$ and it establishes (up to) three linear equations for the wanted components of $\boldsymbol{\alpha}$ and $\boldsymbol{\eta}$. Hence, choosing the number of test fields in accordance with the number of the wanted tensor components, and specifying the geometry of the test fields "sufficiently independent" from each other, these components can be determined uniquely. In doing so, the amplitude of the test fields clearly drops out (Brandenburg et al. 2008b).

Is the result affected by the *geometry* of the test fields? An ansatz like Eq. (7) is in general not exhaustive, but restricted in its validity to a certain class of mean fields, here strictly speaking to stationary fields which change at most linearly in space. Consequently, the geometry of the test fields is without relevance just as long as they are taken from the class for which the $\overline{\boldsymbol{\mathcal{E}}}$ ansatz is valid, but not for other choices.

For many applications it will be useful to generalize the test-field method such that all employed test fields are harmonic functions of position, defined by one and the same wavevector $\boldsymbol{k}$. The turbulent transport coefficients can then be obtained as functions of $\boldsymbol{k}$ and have to be identified with the Fourier transforms of integral kernels which define the in general non-local relationship between $\overline{\boldsymbol{\mathcal{E}}}$ and $\overline{\boldsymbol{B}}$ (Brandenburg et al. 2008a). Quite analogously, the in general also non-instantaneous relationship between these quantities can be recovered by using harmonic functions of time for the test fields. The coefficients, then depending on the angular frequency ω, represent again Fourier transforms of the corresponding integral kernels (Hubbard & Brandenburg 2009).

If $\boldsymbol{u}$ and $\overline{\boldsymbol{U}}$ are taken from a series of main runs with a dynamically effective mean field of, say, fixed geometry, but from run to run differing strength $\overline{B}$, $\boldsymbol{\alpha}$ and $\boldsymbol{\eta}$ can be obtained as functions of $\overline{B}$. Thus, it is possible to determine the *quenched* dynamo coefficients basically in the same way as in the kinematic case, albeit at the cost of multiple numerical work.

Let us now relax the above assumption on the background turbulence and admit additionally a primary *magnetic* turbulence $\boldsymbol{b}_0$. For the sake of simplicity we will not deal here with $\overline{\boldsymbol{\mathcal{E}}}_0$, so let us assume that it vanishes. In the representation Eq. (2) of $\overline{\boldsymbol{\mathcal{E}}}_{\overline{B}}$ we now combine the first and last terms using $\boldsymbol{u} = \boldsymbol{u}_0 + \boldsymbol{u}_{\overline{B}}$ and obtain

$$\overline{\boldsymbol{\mathcal{E}}}_{\overline{B}} = \overline{\boldsymbol{u} \times \boldsymbol{b}_{\overline{B}}} + \overline{\boldsymbol{u}_{\overline{B}} \times \boldsymbol{b}_0}, \tag{8}$$

differing from Eq. (6) by the additional contribution, $\overline{\boldsymbol{u}_{\overline{B}} \times \boldsymbol{b}_0}$. Even when modifying Eq. (5) appropriately to form an equation for $\boldsymbol{b}_{\overline{B}}$, the quasi-kinematic method necessarily fails here as it only provides the term $\overline{\boldsymbol{u} \times \boldsymbol{b}_{\overline{B}}}$. Obviously, a valid scheme must treat also $\boldsymbol{u}_{\overline{B}}$ in a test-field manner similar to $\boldsymbol{b}_{\overline{B}}$. The equation to be employed for $\boldsymbol{u}_{\overline{B}}$ has of course to rely upon the momentum equation. Due to its intrinsic nonlinearity, however, a major challenge consists then in ensuring the linearity and homogeneity of the test solutions in the test fields.

3. A model problem

3.1. Motivation

We commence our study with a model problem that is simpler than the complete MHD setup, but nevertheless shares with it the same mathematical complications. We drop the advection and pressure terms and adopt for the diffusion operator simply the Laplacian (and a homogeneous medium). Thus, there is no constraint on the velocity from the continuity equation and an equation of state. However, as in the full problem, we allow the magnetic field to exert a Lorentz force on the fluid. We also allow for the presence of an imposed uniform magnetic field $\boldsymbol{B}_{\mathrm{imp}}$ to enable a determination of the α effect independently from the test-field method by the imposed-field method.

The magnetic field is hence represented as $\boldsymbol{B} = \boldsymbol{B}_{\mathrm{imp}} + \boldsymbol{\nabla} \times \boldsymbol{A}$, where $\boldsymbol{A}$ is the vector potential of its non-uniform part. The resulting modified momentum equation for the velocity $\boldsymbol{U}$ and the (original) induction equation then read

$$\frac{\partial \boldsymbol{U}}{\partial t} = \boldsymbol{J} \times \boldsymbol{B} + \boldsymbol{F}_{\mathrm{K}} + \nu\nabla^2\boldsymbol{U}, \tag{9}$$

$$\frac{\partial \boldsymbol{A}}{\partial t} = \boldsymbol{U} \times \boldsymbol{B} + \boldsymbol{F}_{\mathrm{M}} + \eta\nabla^2\boldsymbol{A}, \tag{10}$$

where we have included the possibility of both kinetic and magnetic forcing terms, $\boldsymbol{F}_{\mathrm{K}}$ and $\boldsymbol{F}_{\mathrm{M}}$, respectively. (In this paper we use the terms "hydrodynamic forcing" and "kinetic forcing" synonymously.) Furthermore, ν is the kinematic viscosity and η the magnetic diffusivity. We have adopted a system of units in which $\boldsymbol{B}$ has the dimension of velocity. Defining the current density as $\boldsymbol{J} = \boldsymbol{\nabla} \times \boldsymbol{B}$, it has then the unit of inverse time.

As will become clear, the major difficulty in defining a test-field method for an MHD or purely magnetic background turbulence is caused by bilinear (or quadratic) terms like $\boldsymbol{J} \times \boldsymbol{B}$ and $\boldsymbol{U} \times \boldsymbol{B}$. Hence, taking the advective term $\boldsymbol{U} \cdot \boldsymbol{\nabla}\boldsymbol{U}$ into account would not offer any new aspect, but would blur the essence of the derivation and the clear analogy in the treatment of the former two nonlinearities. The treatment of the advective term follows the same pattern, as is demonstrated in Appendix A. Given that our technique is still in its infancy, and that many underlying issues have not been adressed yet, it is a major advantage to begin with the simpler set of equations. This helps significantly in clarifying the approach and in eliminating sources of error in the numerical implementation.

In three dimensions and for $\boldsymbol{B}_{\mathrm{imp}} = \boldsymbol{F}_{\mathrm{M}} = \boldsymbol{0}$, but with kinetic forcing via $\boldsymbol{F}_{\mathrm{K}}$, the system (9), (10) is capable of reproducing essential features of turbulent dynamos like initial exponential growth and subsequent saturation; see, e.g., Brandenburg (2001) or Haugen et al. (2004).

If $\boldsymbol{B}_{\mathrm{imp}} \neq \boldsymbol{0}$ or $\boldsymbol{F}_{\mathrm{M}} \neq \boldsymbol{0}$ we are no longer dealing with a dynamo problem in the strictest sense. A discussion of dynamo processes is still meaningful if $\boldsymbol{B}_{\mathrm{imp}} = \boldsymbol{0}$ and the magnetic forcing does not give rise to a mean electromotive force $\overline{\boldsymbol{\mathcal{E}}}_0$. A possibility to accomplish this is $\boldsymbol{F}_{\mathrm{K}} = \boldsymbol{0}$ together with a magnetic forcing resulting in a Beltrami field $\boldsymbol{b}_0$, but any choice providing an isotropic background turbulence $(\boldsymbol{u}_0, \boldsymbol{b}_0)$ should be suited likewise. Then, in spite of the presence of a magnetic forcing, the *mean-field* induction equation is still autonomous allowing for the solution $\overline{\boldsymbol{B}} = \boldsymbol{0}$. It depends on properties of the background turbulence like chirality whether, e.g., the α effect renders this solution unstable by enabling growing solutions.

If we, however, admit $\boldsymbol{B}_{\mathrm{imp}} \neq \boldsymbol{0}$, at least in the homogeneous case the mean emf, $\boldsymbol{\alpha}\boldsymbol{B}_{\mathrm{imp}}$, is without effect and $\overline{\boldsymbol{B}} = \boldsymbol{B}_{\mathrm{imp}}$ is a solution of the mean-field induction equation which cannot grow.

Should a growing mean field nevertheless be observed, it can so legitimately be attributed to an instability.

Thus, both scenarios for $\boldsymbol{F}_\mathrm{M} \neq \boldsymbol{0}$ have the potential to exhibit *mean-field* dynamos although the original induction equation is inhomogeneous and the dynamo must not be considered as an instability of the completely non-magnetic state. Models of this type may well have astrophysical relevance, because at high magnetic Reynolds numbers small-scale dynamo action is expected to be ubiquitous. Large-scale fields are still considered to be a consequence of an instability, at least if there is no $\overline{\boldsymbol{\mathcal{E}}}_0$ or any other sort of "battery effect". Magnetic forcing can be regarded as a modeling tool for providing a magnetic background turbulence when, e.g., in a DNS the conditions for small-scale dynamo action are not afforded.

Quite generally, magnetic forcing and an imposed field provide excellent means of studying the α effect, the inverse cascade of magnetic helicity, and flow properties in the magnetically dominated regime (see, e.g., Pouquet et al. 1976; Brandenburg et al. 2002; Brandenburg & Käpylä 2007).

3.2. Purely magnetic background turbulence

Before taking on the most general situation of both magnetic and velocity fluctuations in the background, it seems instructive to look first at the case complementary to that discussed in Sect. 2. That is, we assume, perhaps somewhat artificially, that the background velocity fluctuations vanish, i.e. $\boldsymbol{u}_0 = \boldsymbol{0}$, so that $\boldsymbol{u} = \boldsymbol{u}_{\overline{B}}$. According to Eq. (2) we now find

$$\overline{\boldsymbol{\mathcal{E}}} = \overline{\boldsymbol{\mathcal{E}}}_{\overline{B}} = \overline{\boldsymbol{u}_{\overline{B}} \times \boldsymbol{b}} = \overline{\boldsymbol{u} \times \boldsymbol{b}}. \tag{11}$$

The modified momentum equation for the velocity fluctuations in a homogeneous medium reads (cf. Eq. (9))

$$\frac{\partial \boldsymbol{u}}{\partial t} = \overline{\boldsymbol{J}} \times \boldsymbol{b} + \boldsymbol{j} \times \overline{\boldsymbol{B}} + \boldsymbol{\mathcal{F}}' + \nu\nabla^2\boldsymbol{u}, \tag{12}$$

with $\boldsymbol{\mathcal{F}}' = \boldsymbol{j}_{\overline{B}} \times \boldsymbol{b} + \boldsymbol{j}_0 \times \boldsymbol{b}_{\overline{B}} - \overline{\boldsymbol{j}_{\overline{B}} \times \boldsymbol{b}} + \overline{\boldsymbol{j}_0 \times \boldsymbol{b}_{\overline{B}}}$. Here, a prime denotes the departure from the mean value. As $(\boldsymbol{j}_0 \times \boldsymbol{b}_0)'$ needs to vanish in order to guarantee $\boldsymbol{u}_0 = \boldsymbol{0}$, this could also be written as $\boldsymbol{\mathcal{F}}' = \boldsymbol{j} \times \boldsymbol{b} - \overline{\boldsymbol{j} \times \boldsymbol{b}}$. Unlike in the quasi-kinematic method there is now no longer any way to base a test-field method upon considering one of the fluctuating fields, here $\boldsymbol{b}$, to be given (e.g. taken from a main run) while interpreting the other, here $\boldsymbol{u}$, and consequently $\overline{\boldsymbol{\mathcal{E}}}$ as a linear and homogeneous functional of the mean field. (This would work here, however, in the second order correlation approximation, where $\boldsymbol{\mathcal{F}}'$ is set to zero.)

3.3. General mean-field treatment

The mean-field equations for $\overline{\boldsymbol{U}}$ and $\overline{\boldsymbol{B}} = \mathrm{curl}\,\overline{\boldsymbol{A}} + \boldsymbol{B}_\mathrm{imp}$ obtained by averaging Eqs. (9) and (10) are

$$\frac{\partial \overline{\boldsymbol{U}}}{\partial t} = \nu\nabla^2\overline{\boldsymbol{U}} + \overline{\boldsymbol{J}} \times \overline{\boldsymbol{B}} + \overline{\boldsymbol{\mathcal{F}}}, \tag{13}$$

$$\frac{\partial \overline{\boldsymbol{A}}}{\partial t} = \eta\nabla^2\overline{\boldsymbol{A}} + \overline{\boldsymbol{U}} \times \overline{\boldsymbol{B}} + \overline{\boldsymbol{\mathcal{E}}}, \tag{14}$$

where we have assumed that the mean forcing terms vanish. From now on we extend our considerations also to the relation between the mean ponderomotive force $\overline{\boldsymbol{\mathcal{F}}} = \overline{\boldsymbol{j} \times \boldsymbol{b}}$ and the mean field. In analogy to the mean electromotive force we write, to start with,

$$\overline{\boldsymbol{\mathcal{F}}}_{\overline{B}} = \boldsymbol{\phi}\overline{\boldsymbol{B}} - \boldsymbol{\psi}\nabla\overline{\boldsymbol{B}}. \tag{15}$$

In the sense explained above for $\boldsymbol{\alpha}$ and $\boldsymbol{\eta}$ the tensors $\boldsymbol{\phi}$ and $\boldsymbol{\psi}$ may depend on $\overline{\boldsymbol{B}}$. For a discussion of the completeness of the ansatz (15), see Appendix B.

In the kinematic limit $\boldsymbol{\phi}$ and $\boldsymbol{\psi}$ are expected to be non-vanishing only if $\boldsymbol{b}_0 \neq \boldsymbol{0}$. An analysis in SOCA, however, would also require $\boldsymbol{u}_0 \neq \boldsymbol{0}$ to get a non-vanishing result; see Appendix C. Note that $\boldsymbol{b}_0 \neq \boldsymbol{0}$ allows $\overline{\boldsymbol{\mathcal{F}}}_{\overline{B}}$ to be linear in $\overline{\boldsymbol{B}}$, which would otherwise be quadratic to leading order. Consequently, the back-reaction of the mean field onto the flow is no longer independent of its sign.

As $\overline{\boldsymbol{\mathcal{F}}}_{\overline{B}}$ is the divergence of the mean Maxwell tensor, it has to vanish in the homogeneous case, i.e. for homogeneous turbulence and a uniform mean field. Hence, for Eq. (15) to be valid in physical space, $\boldsymbol{\phi}$ has then to vanish. However, in Fourier space we may retain relation (15) with $\lim_{k\to 0}\boldsymbol{\phi}(\boldsymbol{k}) = \boldsymbol{0}$ (but not so for $\boldsymbol{\psi}$). On the other hand, in physical space a description of $\overline{\boldsymbol{\mathcal{F}}}_{\overline{B}}$ employing the second derivatives of $\overline{\boldsymbol{B}}$ is likely to be more appropriate, i.e.

$$\overline{\boldsymbol{\mathcal{F}}}_{\overline{B}} = \boldsymbol{\phi}^*\nabla(\nabla\overline{\boldsymbol{B}}) - \boldsymbol{\psi}\nabla\overline{\boldsymbol{B}}. \tag{16}$$

According to the expression for $\boldsymbol{\phi}(\boldsymbol{k})$, which is derived in Appendix C for Roberts forcing, Eq. (16) specified to

$$\overline{\boldsymbol{\mathcal{F}}}_{\overline{B}} = \boldsymbol{\phi}^*\frac{\partial^2\overline{\boldsymbol{B}}}{\partial z^2} - \boldsymbol{\psi}\overline{\boldsymbol{J}}$$

would indeed be sufficient as long as there is sufficient scale separation between mean and fluctuating fields. In the following, we continue referring to $\boldsymbol{\phi}$ as introduced by Eq. (15).

The equations for the fluctuations are obtained by subtracting Eqs. (13) from (9), and Eq. (14) from (10), what leads to

$$\frac{\partial \boldsymbol{u}}{\partial t} = \overline{\boldsymbol{J}} \times \boldsymbol{b} + \boldsymbol{j} \times \overline{\boldsymbol{B}} + \boldsymbol{\mathcal{F}}' + \boldsymbol{f}_\mathrm{K} + \nu\nabla^2\boldsymbol{u}, \tag{17}$$

$$\frac{\partial \boldsymbol{a}}{\partial t} = \overline{\boldsymbol{U}} \times \boldsymbol{b} + \boldsymbol{u} \times \overline{\boldsymbol{B}} + \boldsymbol{\mathcal{E}}' + \boldsymbol{f}_\mathrm{M} + \eta\nabla^2\boldsymbol{a}, \tag{18}$$

respectively, where $\boldsymbol{\mathcal{F}}' = \boldsymbol{j} \times \boldsymbol{b} - \overline{\boldsymbol{j} \times \boldsymbol{b}}$ and $\boldsymbol{\mathcal{E}}' = \boldsymbol{u} \times \boldsymbol{b} - \overline{\boldsymbol{u} \times \boldsymbol{b}}$ are terms that are quadratic in the correlations, while $\boldsymbol{f}_\mathrm{K,M}$ are just the fluctuating parts of the forcing functions.

Our aim is now to derive a set of formally linear equations whose solutions, considered as responses to a given mean field, are linear and homogeneous in the latter. For this purpose we make use of the split of all quantities into parts existing in the absence of $\overline{\boldsymbol{B}}$ and parts vanishing with $\overline{\boldsymbol{B}}$, as introduced in Sect. 2. We write $\boldsymbol{u} = \boldsymbol{u}_0 + \boldsymbol{u}_{\overline{B}}$, $\boldsymbol{a} = \boldsymbol{a}_0 + \boldsymbol{a}_{\overline{B}}$ and $\boldsymbol{j} = \boldsymbol{j}_0 + \boldsymbol{j}_{\overline{B}}$, as well as $\boldsymbol{\mathcal{F}}' = \boldsymbol{\mathcal{F}}'_0 + \boldsymbol{\mathcal{F}}'_{\overline{B}}$ and $\boldsymbol{\mathcal{E}}' = \boldsymbol{\mathcal{E}}'_0 + \boldsymbol{\mathcal{E}}'_{\overline{B}}$, and assume that the forcing is independent of $\overline{\boldsymbol{B}}$. Equations (17) and (18) split consequently as follows (see Appendix D for an illustration)

$$\frac{\partial \boldsymbol{u}_0}{\partial t} = \nu\nabla^2\boldsymbol{u}_0 + \boldsymbol{\mathcal{F}}'_0 + \boldsymbol{f}_\mathrm{K}, \tag{19}$$

$$\frac{\partial \boldsymbol{a}_0}{\partial t} = \eta\nabla^2\boldsymbol{a}_0 + \overline{\boldsymbol{U}} \times \boldsymbol{b}_0 + \boldsymbol{\mathcal{E}}'_0 + \boldsymbol{f}_\mathrm{M}, \tag{20}$$

$$\frac{\partial \boldsymbol{u}_{\overline{B}}}{\partial t} = \nu\nabla^2\boldsymbol{u}_{\overline{B}} + \overline{\boldsymbol{J}} \times \boldsymbol{b} + \boldsymbol{j} \times \overline{\boldsymbol{B}} + \boldsymbol{\mathcal{F}}'_{\overline{B}}, \tag{21}$$

$$\frac{\partial \boldsymbol{a}_{\overline{B}}}{\partial t} = \eta\nabla^2\boldsymbol{a}_{\overline{B}} + \overline{\boldsymbol{U}} \times \boldsymbol{b}_{\overline{B}} + \boldsymbol{u} \times \overline{\boldsymbol{B}} + \boldsymbol{\mathcal{E}}'_{\overline{B}}. \tag{22}$$

Because of $\boldsymbol{\mathcal{F}}'_0 = (\boldsymbol{j}_0 \times \boldsymbol{b}_0)'$ and $\boldsymbol{\mathcal{E}}'_0 = (\boldsymbol{u}_0 \times \boldsymbol{b}_0)'$, Eqs. (19) and (20) are completely closed. Furthermore, we have

$$\boldsymbol{\mathcal{F}}'_{\overline{B}} = (\boldsymbol{j}_0 \times \boldsymbol{b}_{\overline{B}} + \boldsymbol{j}_{\overline{B}} \times \boldsymbol{b}_0 + \boldsymbol{j}_{\overline{B}} \times \boldsymbol{b}_{\overline{B}})', \tag{23}$$

$$\boldsymbol{\mathcal{E}}'_{\overline{B}} = (\boldsymbol{u}_0 \times \boldsymbol{b}_{\overline{B}} + \boldsymbol{u}_{\overline{B}} \times \boldsymbol{b}_0 + \boldsymbol{u}_{\overline{B}} \times \boldsymbol{b}_{\overline{B}})'. \tag{24}$$

We can rewrite these expressions such that they become formally linear in $\boldsymbol{u}_{\overline{B}}$ and $\boldsymbol{b}_{\overline{B}}$, each in two different flavors:

$$\mathcal{F}'_{\overline{B}} = (\boldsymbol{j}\times\boldsymbol{b}_{\overline{B}} + \boldsymbol{j}_{\overline{B}}\times\boldsymbol{b}_0)' = (\boldsymbol{j}_0\times\boldsymbol{b}_{\overline{B}} + \boldsymbol{j}_{\overline{B}}\times\boldsymbol{b})', \tag{25}$$

$$\mathcal{E}'_{\overline{B}} = (\boldsymbol{u}\times\boldsymbol{b}_{\overline{B}} + \boldsymbol{u}_{\overline{B}}\times\boldsymbol{b}_0)' = (\boldsymbol{u}_0\times\boldsymbol{b}_{\overline{B}} + \boldsymbol{u}_{\overline{B}}\times\boldsymbol{b})'. \tag{26}$$

Now we have achieved our goal of deriving a system of formally linear equations defining the parts of the fluctuations that can be related to the mean field as response to its interaction with the given fluctuating fields $\boldsymbol{u}$, $\boldsymbol{u}_0$, $\boldsymbol{b}$, and $\boldsymbol{b}_0$.

For the parts of the mean ponderomotive and electromotive forces existing already with $\overline{\boldsymbol{B}} = \boldsymbol{0}$ we find

$$\overline{\mathcal{F}}_0 = \overline{\boldsymbol{j}_0\times\boldsymbol{b}_0} \quad\text{and}\quad \overline{\mathcal{E}}_0 = \overline{\boldsymbol{u}_0\times\boldsymbol{b}_0} \tag{27}$$

which could be finite due to a small-scale dynamo or magnetic forcing. Although it is hard to imagine that isotropic forcing alone is capable of enabling a non-vanishing $\overline{\mathcal{F}}_0$ or $\overline{\mathcal{E}}_0$, an additional vector influencing the otherwise isotropic turbulence may well act in this way. For example, using the second-order correlation approximation (SOCA) it was found that in the presence of a non-uniform mean flow $\overline{\boldsymbol{U}}$ with mean vorticity $\overline{\boldsymbol{W}} = \mathrm{curl}\,\overline{\boldsymbol{U}}$ we have, in ideal MHD ($\eta = \nu = 0$),

$$\overline{\mathcal{E}}_0 = -\frac{\tau_U}{3}\,\overline{\boldsymbol{u}_{00}\cdot\boldsymbol{j}_{00}}\,\overline{\boldsymbol{U}} + \frac{\tau_W}{3}\,\overline{\boldsymbol{u}_{00}\cdot\boldsymbol{b}_{00}}\,\overline{\boldsymbol{W}}. \tag{28}$$

Here the index "00" refers to the fluctuating background uninfluenced by *both* the magnetic field and the mean flow. Beyond this specific result, too, one may expect that quite general some cross correlation of the primary turbulences is crucial. (Yoshizawa 1990; Rädler & Brandenburg 2010).

For the parts vanishing with $\overline{\boldsymbol{B}}$ we have

$$\overline{\mathcal{F}}_{\overline{B}} = \overline{\boldsymbol{j}\times\boldsymbol{b}_{\overline{B}}} + \overline{\boldsymbol{j}_{\overline{B}}\times\boldsymbol{b}_0} = \overline{\boldsymbol{j}_0\times\boldsymbol{b}_{\overline{B}}} + \overline{\boldsymbol{j}_{\overline{B}}\times\boldsymbol{b}}, \tag{29}$$

$$\overline{\mathcal{E}}_{\overline{B}} = \overline{\boldsymbol{u}\times\boldsymbol{b}_{\overline{B}}} + \overline{\boldsymbol{u}_{\overline{B}}\times\boldsymbol{b}_0} = \overline{\boldsymbol{u}_0\times\boldsymbol{b}_{\overline{B}}} + \overline{\boldsymbol{u}_{\overline{B}}\times\boldsymbol{b}}. \tag{30}$$

We recall that for $\boldsymbol{b}_0 = \boldsymbol{0}$ (see Sect. 2), only the term $\overline{\boldsymbol{u}\times\boldsymbol{b}_{\overline{B}}} \equiv \overline{\mathcal{E}}^{\mathrm{K}}_{\overline{B}}$ occurs in the mean electromotive force and for $\boldsymbol{u}_0 = \boldsymbol{0}$ (see Eq. (11)) only $\overline{\boldsymbol{u}_{\overline{B}}\times\boldsymbol{b}} \equiv \overline{\mathcal{E}}^{\mathrm{M}}_{\overline{B}}$. For interpretation purposes it is therefore convenient to define correspondingly symmetrized versions of (29) and (30),

$$\overline{\mathcal{F}}_{\overline{B}} = \overline{\boldsymbol{j}\times\boldsymbol{b}_{\overline{B}}} + \overline{\boldsymbol{j}_{\overline{B}}\times\boldsymbol{b}} - \overline{\boldsymbol{j}_{\overline{B}}\times\boldsymbol{b}_{\overline{B}}} = \overline{\mathcal{F}}^{\mathrm{K}}_{\overline{B}} + \overline{\mathcal{F}}^{\mathrm{M}}_{\overline{B}} + \overline{\mathcal{F}}^{\mathrm{R}}_{\overline{B}}$$

$$\overline{\mathcal{E}}_{\overline{B}} = \overline{\boldsymbol{u}\times\boldsymbol{b}_{\overline{B}}} + \overline{\boldsymbol{u}_{\overline{B}}\times\boldsymbol{b}} - \overline{\boldsymbol{u}_{\overline{B}}\times\boldsymbol{b}_{\overline{B}}} = \overline{\mathcal{E}}^{\mathrm{K}}_{\overline{B}} + \overline{\mathcal{E}}^{\mathrm{M}}_{\overline{B}} + \overline{\mathcal{E}}^{\mathrm{R}}_{\overline{B}},$$

with $\overline{\mathcal{F}}^{\mathrm{R}}_{\overline{B}} = -\overline{\boldsymbol{j}_{\overline{B}}\times\boldsymbol{b}_{\overline{B}}}$ and $\overline{\mathcal{E}}^{\mathrm{R}}_{\overline{B}} = -\overline{\boldsymbol{u}_{\overline{B}}\times\boldsymbol{b}_{\overline{B}}}$ being residual terms. Of course this split is only meaningful with a non-vanishing mean field in the main run. The corresponding transport coefficients might be split analogously. However, for an imposed field in, say, the i direction this is restricted to the (ij) components of the tensors.

3.4. Test-field method

In a next step we define the actual test equations starting from Eqs. (21), (22), (25) and (26). As they are already arranged to be formally linear when deliberately ignoring the relations between $\boldsymbol{u}_{\overline{B}}$ and $\boldsymbol{u}$ as well as between $\boldsymbol{b}_{\overline{B}}$ and $\boldsymbol{b}$, respectively, we have nothing more to do than to identify $\overline{\boldsymbol{B}}$ with a test field $\overline{\boldsymbol{B}}^{\mathrm{T}}$ and $(\boldsymbol{u}_{\overline{B}}, \boldsymbol{b}_{\overline{B}})$ with the corresponding test solution $(\boldsymbol{u}^{\mathrm{T}}, \boldsymbol{b}^{\mathrm{T}})$. Due to the ambiguity in Eqs. (25) and (26) four different versions are obtained reading

Table 1. The four versions of the generalized test-field method as generated by combining the different representations of $\mathcal{F}^{\mathrm{T}\prime}$ and $\mathcal{E}^{\mathrm{T}\prime}$ in Eqs. (33) and (34).

	$\boldsymbol{j}\times\boldsymbol{b}^{\mathrm{T}} + \boldsymbol{j}^{\mathrm{T}}\times\boldsymbol{b}_0$	$\boldsymbol{j}_0\times\boldsymbol{b}^{\mathrm{T}} + \boldsymbol{j}^{\mathrm{T}}\times\boldsymbol{b}$
$\boldsymbol{u}\times\boldsymbol{b}^{\mathrm{T}} + \boldsymbol{u}^{\mathrm{T}}\times\boldsymbol{b}_0$	ju	bu
$\boldsymbol{u}_0\times\boldsymbol{b}^{\mathrm{T}} + \boldsymbol{u}^{\mathrm{T}}\times\boldsymbol{b}$	jb	bb

$$\frac{\partial\boldsymbol{u}^{\mathrm{T}}}{\partial t} = \overline{\boldsymbol{J}}^{\mathrm{T}}\times\boldsymbol{b} + \boldsymbol{j}\times\overline{\boldsymbol{B}}^{\mathrm{T}} + \mathcal{F}^{\mathrm{T}\prime} + \nu\nabla^2\boldsymbol{u}^{\mathrm{T}}, \tag{31}$$

$$\frac{\partial\boldsymbol{a}^{\mathrm{T}}}{\partial t} = \overline{\boldsymbol{U}}\times\boldsymbol{b}^{\mathrm{T}} + \boldsymbol{u}\times\overline{\boldsymbol{B}}^{\mathrm{T}} + \mathcal{E}^{\mathrm{T}\prime} + \eta\nabla^2\boldsymbol{a}^{\mathrm{T}}, \tag{32}$$

with

$$\mathcal{F}^{\mathrm{T}\prime} = \begin{cases} (\boldsymbol{j}\times\boldsymbol{b}^{\mathrm{T}} + \boldsymbol{j}^{\mathrm{T}}\times\boldsymbol{b}_0)' \\ \text{or} \\ (\boldsymbol{j}_0\times\boldsymbol{b}^{\mathrm{T}} + \boldsymbol{j}^{\mathrm{T}}\times\boldsymbol{b})', \end{cases} \tag{33}$$

$$\mathcal{E}^{\mathrm{T}\prime} = \begin{cases} (\boldsymbol{u}\times\boldsymbol{b}^{\mathrm{T}} + \boldsymbol{u}^{\mathrm{T}}\times\boldsymbol{b}_0)' \\ \text{or} \\ (\boldsymbol{u}_0\times\boldsymbol{b}^{\mathrm{T}} + \boldsymbol{u}^{\mathrm{T}}\times\boldsymbol{b})'. \end{cases} \tag{34}$$

Correspondingly we express the mean ponderomotive and electromotive forces by the test solutions as

$$\overline{\mathcal{F}}^{\mathrm{T}} = \begin{cases} \overline{\boldsymbol{j}\times\boldsymbol{b}^{\mathrm{T}}} + \overline{\boldsymbol{j}^{\mathrm{T}}\times\boldsymbol{b}_0} \\ \text{or} \\ \overline{\boldsymbol{j}_0\times\boldsymbol{b}^{\mathrm{T}}} + \overline{\boldsymbol{j}^{\mathrm{T}}\times\boldsymbol{b}}, \end{cases} \tag{35}$$

$$\overline{\mathcal{E}}^{\mathrm{T}} = \begin{cases} \overline{\boldsymbol{u}\times\boldsymbol{b}^{\mathrm{T}}} + \overline{\boldsymbol{u}^{\mathrm{T}}\times\boldsymbol{b}_0} \\ \text{or} \\ \overline{\boldsymbol{u}_0\times\boldsymbol{b}^{\mathrm{T}}} + \overline{\boldsymbol{u}^{\mathrm{T}}\times\boldsymbol{b}}, \end{cases} \tag{36}$$

and stipulate that the choice within Eqs. (35) and (36) is always to correspond to the choice in Eqs. (33) and (34). As we will make use of all four possible versions we label them in a unique way by the names of the fluctuating fields of the main run that enter the expressions for $\mathcal{F}^{\mathrm{T}\prime}$ and $\mathcal{E}^{\mathrm{T}\prime}$. Accordingly, we find by inspection of Eqs. (33) and (34) for the labels the combinations ju, jb, bu and bb; see Table 1.

Now we conclude that for given $\boldsymbol{u}$, $\boldsymbol{b}$, $\boldsymbol{u}_0$, $\boldsymbol{b}_0$ and $\overline{\boldsymbol{U}}$ the test solutions $\boldsymbol{u}^{\mathrm{T}}$ and $\boldsymbol{b}^{\mathrm{T}}$ are linear and homogeneous in the test fields $\overline{\boldsymbol{B}}^{\mathrm{T}}$ and that the same holds for $\overline{\mathcal{F}}^{\mathrm{T}}$ and $\overline{\mathcal{E}}^{\mathrm{T}}$. Hence, the tensors $\boldsymbol{\alpha}$, $\boldsymbol{\eta}$, $\boldsymbol{\phi}$ and $\boldsymbol{\psi}$ derived from these quantities will not depend on the test fields, but exclusively reflect properties of the given fluctuating fields and the mean velocity. If these are affected by a mean field in the main run the tensor components will show a dependence on $\overline{B}$. Thus, like in the quasi-kinematic method, quenching behavior can be identified. We observe further that, when using the mean field from the main run as one of the test fields, the corresponding test solutions $\boldsymbol{b}^{\mathrm{T}}$ and $\boldsymbol{u}^{\mathrm{T}}$ will coincide with $\boldsymbol{b}_{\overline{B}}$ and $\boldsymbol{u}_{\overline{B}}$, respectively.

Summing up, we may claim that the presented generalized test-field method in either shape satisfies certain necessary conditions for the correctness of its results. But can we be confident, that these are sufficient? An obvious complication lies in the fact that, in contrast to the quasi-kinematic method yielding the transport coefficients uniquely, we have now to deal with four different versions which need not be equivalent. Indeed we will demonstrate that the reformulation of the original problem into Eqs. (31) and (32) with Eqs. (33) and (34) introduces spurious instabilities in some applications. As we presently see no strict mathematical argument for the identity of the outcomes of all four versions, we resort to an empirical justification of our approach. This is what the rest of this paper mainly is devoted to.

Remarks: (i) Applying the second order correlation approximation (SOCA) to the system (31), (32), that is, neglecting $\boldsymbol{\mathcal{F}}^{\mathrm{T}\prime}$ and $\boldsymbol{\mathcal{E}}^{\mathrm{T}\prime}$, melts the four versions down to one and thus removes any ambiguities.
(ii) In the kinematic limit $\overline{\boldsymbol{B}} \rightarrow \boldsymbol{0}$ we have simultaneously $\boldsymbol{u} \rightarrow \boldsymbol{u}_0$ and $\boldsymbol{b} \rightarrow \boldsymbol{b}_0$, so again only one version remains. The method has then of course no longer any value for quenching considerations, but it still might be useful to overcome the limitations of SOCA.
(iii) For $\boldsymbol{b}_0 = \boldsymbol{0}$, Eq. (32) with the first version of Eq. (34), i.e.

$$\boldsymbol{\mathcal{E}}^{\mathrm{T}\prime} = (\boldsymbol{u} \times \boldsymbol{b}_T)', \tag{37}$$

and correspondingly $\overline{\boldsymbol{\mathcal{E}}}^{\mathrm{T}} = \overline{\boldsymbol{u} \times \boldsymbol{b}_T}$, but (31) ignored, reverts to the quasi-kinematic method. For comparison we will occasionally apply this method even when $\boldsymbol{b}_0 \neq \boldsymbol{0}$ and label the quantities calculated in this way with an upper index "QK".

From now on we define mean fields by averaging over two directions, here over all x and y, that is, all mean quantities depend merely on z (if at all) and we obtain a 1D mean-field dynamo problem. As a consequence, $\overline{B}_z$ is constant and there are only two non-vanishing components of $\boldsymbol{\nabla}\overline{\boldsymbol{B}}$, namely $\overline{J}_x$ and $\overline{J}_y$ so only the evolution of $\overline{B}_x$ and $\overline{B}_y$ has to be considered. Moreover, $\overline{\mathcal{E}}_z$ is without influence on the evolution of $\overline{\boldsymbol{B}}$. Hence, instead of Eqs. (15) and (7) we can write

$$\overline{\mathcal{F}}_i = \phi_{ij}\overline{B}_j - \psi_{ij}\overline{J}_j, \quad \overline{\mathcal{E}}_i = \alpha_{ij}\overline{B}_j - \eta_{ij}\overline{J}_j, \tag{38}$$

where the original rank-three tensors $\boldsymbol{\psi}$ and $\boldsymbol{\eta}$ are degenerated to rank-two ones.

Only the four components of either tensor with $i, j = 1, 2$ are of interest, thus altogether 16 components need to be determined. As one test field $\overline{\boldsymbol{B}}^{\mathrm{T}}$ comprises two relevant components and yields one $\overline{\boldsymbol{\mathcal{F}}}^{\mathrm{T}}$ and one $\overline{\boldsymbol{\mathcal{E}}}^{\mathrm{T}}$, each again with two relevant components, we need to consider solutions of (31) through (34) for a set of four different test fields.

Selection of test fields: The simplest choice are uniform fields in the x and y directions, but they are only suited to determine the $\boldsymbol{\alpha}$ tensor.

All four tensors can be extracted by use of test fields with either the x or the y component proportional to either $\cos k_z z$ or $\sin k_z z$ and the other vanishing (see, e.g., Brandenburg 2005b; Brandenburg et al. 2008a, 2008b; Sur et al. 2008). That is, $\overline{\boldsymbol{B}}^{\mathrm{T}}$ is either $B_i^{pc} = \delta_{ip} \cos k_z z$ or $B_i^{ps} = \delta_{ip} \sin k_z z$, where the superscript pq with $p = 1, 2$ and $q = \mathrm{c}, \mathrm{s}$ labels the test field. The wavenumber k_z is bounded from below by $2\pi/L_z$, where L_z is the extent of the computational domain in the z direction. By varying k_z, the wanted tensor components can be determined as functions of k_z. They have then no longer to be interpreted in the usual way, but as Fourier transforms of integral kernels instead (cf. Brandenburg et al. 2008a). In other terms, as the harmonic test fields do not belong to the class of mean fields for which the ansatzes (7) and (15) are exhaustive (see Sect. 2) we must be aware that the tensors calculated in this way are "polluted" by contributions from terms with higher spatial derivatives of $\overline{\boldsymbol{B}}$.

For each pair of test fields $(\overline{\boldsymbol{B}}^{p\mathrm{c}}, \overline{\boldsymbol{B}}^{p\mathrm{s}})$ we determine 2×4 unknowns by solving the linear systems

$$\overline{\mathcal{F}}_i^{pq} = \phi_{ij}\overline{B}_j^{pq} - \psi_{ij}\overline{J}_j^{pq}, \quad \overline{\mathcal{E}}_i^{pq} = \alpha_{ij}\overline{B}_j^{pq} - \eta_{ij}\overline{J}_j^{pq}, \tag{39}$$

$q = \mathrm{c,s}$. Note that there is no coupling between the systems for $p = 1$ and $p = 2$. Both coefficient matrices in (39) are given by the rotation matrix

$$\mathsf{R} = \begin{pmatrix} \cos k_z z & -\sin k_z z \\ \sin k_z z & \cos k_z z \end{pmatrix} \tag{40}$$

(with the angle $k_z z$) and the solutions are

$$\begin{pmatrix} \phi_{ij} \\ \psi_{ij} k_z \end{pmatrix} = \mathsf{R}^{\mathrm{t}} \begin{pmatrix} \overline{\mathcal{F}}_i^{jc} \\ \overline{\mathcal{F}}_i^{js} \end{pmatrix}, \quad \begin{pmatrix} \alpha_{ij} \\ \eta_{ij} k_z \end{pmatrix} = \mathsf{R}^{\mathrm{t}} \begin{pmatrix} \overline{\mathcal{E}}_i^{jc} \\ \overline{\mathcal{E}}_i^{js} \end{pmatrix}. \tag{41}$$

Here the superscript "t" indicates transposition.

3.5. Forcing functions, computational domain, and boundary conditions

For testing purposes, a common and convenient choice is the Roberts flow forcing function,

$$\boldsymbol{f} = \sigma k_{\mathrm{f}} \Psi \hat{\boldsymbol{z}} + \boldsymbol{\nabla} \times (\Psi \hat{\boldsymbol{z}}) \quad \text{with} \quad \Psi = \cos k_x x \cos k_y y, \tag{42}$$

and the effective forcing wavenumber $k_{\mathrm{f}} = (k_x^2 + k_y^2)^{1/2}$. With the chosen averaging the Roberts forcing is isotropic in the xy plane. Furthermore, σ is a parameter controlling the helicity of the forcing: with $\sigma = 0$ it is non-helical while for $\sigma = 1$ it reaches maximum helicity. If not declared otherwise, we will employ maximally helical Roberts forcing. We choose here $k_x = k_y = k_1$ where k_1 is the smallest wavenumber that fits into the x and y extent of the computational domain (see below).

The Roberts forcing function will be employed for kinetic as well as magnetic forcing, so we write $\boldsymbol{f}_{\mathrm{K,M}} = N_{\mathrm{K,M}} \boldsymbol{f}$, where the $N_{\mathrm{K,M}}$ are amplitudes having the units of acceleration and velocity squared, respectively. Note that for $\sigma = 1$, Eq. (42) yields a Beltrami field, i.e., it has the property $\mathrm{curl}\, \boldsymbol{f} = k_{\mathrm{f}} \boldsymbol{f}$. Provided $\boldsymbol{B}_{\mathrm{imp}} = \boldsymbol{0}$, the kinetic and magnetic forcings act completely uninfluenced from each other because a $\boldsymbol{b}_0$ with Beltrami property exerts no Lorentz force and $\boldsymbol{u}_0 \propto \boldsymbol{b}_0$. Thus, a flow and a magnetic field are created that have exact Roberts geometry. This is not the case for $\sigma \neq 1$, because then the Beltrami property is not obeyed.

The computational domain is a cuboid with quadratic base $L_x = L_y = 2\pi$ while its z extent remains adjustable and depends on the smallest wavenumber in the z direction, k_z, to be considered. However, as the Roberts forcing function is not z dependent, the runs from which only $\boldsymbol{\alpha}$ is extracted were carried out in 2D with $k_z = 0$. In all cases we assume periodic boundary conditions in all directions.

The results presented below were obtained using revision `r13439` of the Pencil Code[1], which is a modular high-order code (sixth order in space and third-order in time) for solving a large range of different partial differential equations.

[1] http://pencil-code.googlecode.com

3.6. Control parameters and non-dimensionalization

In cases with an imposed magnetic field, we set $\boldsymbol{B}_{\rm imp} = (B_0, 0, 0)$. Along with B_0, the forcing amplitudes $N_{\rm K,M}$ are the most relevant control parameters. The only remaining one is the magnetic Prandtl number, ${\rm Pr_M} = \nu/\eta$. If not otherwise specified it is set to unity, i.e. $\nu = \eta$.

It is convenient to measure length in units of the inverse minimal wavenumber k_1, time in units of $1/\eta k_1^2$, velocity in units of ηk_1, just as the magnetic field. The forcing amplitudes $N_{\rm K,M}$ are given in units of $\eta^2 k_1^3$ and $\eta^2 k_1^2$, respectively. Results will also be presented in dimensionless form: α_{ij} and ψ_{ij} in units of ηk_1, η_{ij} in units of η, and ϕ_{ij} in units of ηk_1^2, if not declared otherwise. Dimensionless quantities are denoted by a tilde throughout.

The intensities of the actual and background turbulences are readily measured by the magnetic Reynolds and Lundquist numbers,

$$ {\rm Re_M} = u_{\rm rms}/\eta k_{\rm f}, \quad {\rm Lu} = b_{\rm rms}/\eta k_{\rm f}, \tag{43} $$

where $u_{\rm rms}$ and $b_{\rm rms}$ are the rms values of fluctuating velocity and magnetic field, respectively.

4. Results

An important criterion for the correctness of the generalized test-field methods is the agreement of their results with those of the imposed-field method which is, of course, only applicable if the actual mean field in the main run is uniform. In most cases we checked for this criterion, the being restricted to $k_z = 0$ in the test fields. On the other hand, in many cases with vanishing $\overline{\boldsymbol{B}}$, but $k_z \neq 0$ we were still able to perform validation by comparing with analytical results.

Due to the properties of the Roberts forcing we have $\overline{\boldsymbol{\mathcal{F}}}_0 = \overline{\boldsymbol{\mathcal{E}}}_0 = \boldsymbol{0}$ throughout. For this reason, and because in the main runs no other mean fields than the uniform occurred, the mean flow $\overline{\boldsymbol{U}}$ is vanishing too.

4.1. Limit of vanishing mean magnetic field

In this section we assume that the mean field is absent or weak enough so as not to affect the fluctuating fields markedly, that is, $\boldsymbol{u} \approx \boldsymbol{u}_0$, $\boldsymbol{b} \approx \boldsymbol{b}_0$. In particular, it can then not render the transport coefficients anisotropic. Therefore, we denote by α and $\eta_{\rm t}$ simply the average of the first two diagonal components of $\boldsymbol{\alpha}$ and $\boldsymbol{\eta}$, i.e. $\alpha = (\alpha_{11} + \alpha_{22})/2$ and $\eta_{\rm t} = (\eta_{11} + \eta_{22})/2$, respectively. If not specified otherwise we set $\widetilde{B}_{\rm imp} = 10^{-3}$ or zero.

4.1.1. Purely hydrodynamic forcing

In order to make contact with known results, we consider first the case of the hydrodynamically driven Roberts flow. In two dimensions, no small-scale dynamo is possible, hence $\boldsymbol{b}_0 = \boldsymbol{0}$ and $u_{0\rm rms} = N_{\rm K}/\nu k_{\rm f}^2$. In three dimensions, however, this solution could be unstable, allowing in particular for a $\boldsymbol{b}_0 \neq \boldsymbol{0}$, but we have not yet employed sufficiently large ${\rm Re_M}$ for that to occur. For ${\rm Re_M} \ll 1$, α is given by (Brandenburg et al. 2008a)

$$ \alpha/\alpha_{0\rm K} = {\rm Re_M}/[1 + (k_z/k_{\rm f})^2], \quad \alpha_{0\rm K} = -u_{\rm rms}/2, \tag{44} $$

where k_z is the wavenumber of the harmonic test fields. The minus sign in $\alpha_{0\rm K}$ accounts for the fact that the Roberts flow has for $\sigma > 0$ positive helicity, which results in a negative α.

Making use of the quasi-kinematic method, as well as of all four versions of the generalized method, we calculated α for $N_{\rm M} = 0$, $k_z = 0$ (2D case) and values of $\tilde{N}_{\rm K}$ ranging from 0.01 to 100 with a ratio of 10, where $\tilde{u}_{\rm rms}$ grows then from 0.005 to 50. Figure 1 shows α/α_0 versus ${\rm Re_M}$ (solid line). Here the data points for all methods are indistinguishable and agree also with those of the imposed-field method.

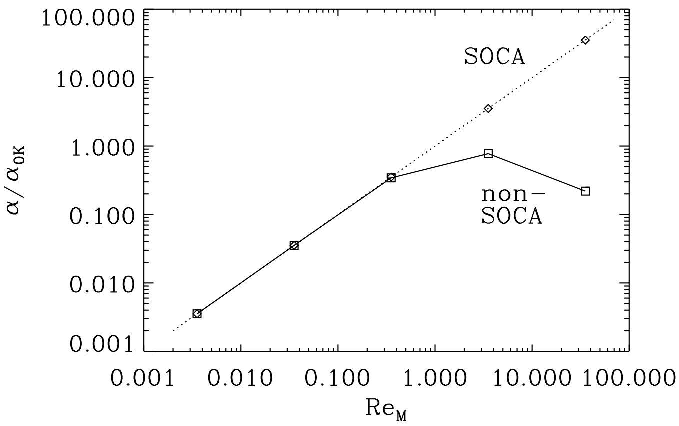

Fig. 1. $\alpha/\alpha_{0\rm K}$ vs. ${\rm Re_M}$ for purely kinetic Roberts forcing with $k_z = 0$ (2D case) from the quasi-kinematic and all versions of the generalized method (solid line with squares). Note the full agreement with Eq. (44) (dotted line) for ${\rm Re_M} \ll 1$. Diamonds: results of the generalized methods with $\boldsymbol{\mathcal{F}}^{\rm T\prime}$ and $\boldsymbol{\mathcal{E}}^{\rm T\prime}$ in Eqs. (31) and (32) neglected, again coinciding with Eq. (44).

Agreement with the SOCA result Eq. (44) (dotted line) exists for ${\rm Re_M} \ll 1$. For ${\rm Re_M} > 1$, SOCA is not applicable, because dropping the $\boldsymbol{\mathcal{E}}^{\rm T\prime}$ term in (32) is then no longer justified. The SOCA values are nevertheless numerically reproducible by the test-field methods when ignoring the $\boldsymbol{\mathcal{F}}^{\rm T\prime}$ and $\boldsymbol{\mathcal{E}}^{\rm T\prime}$ terms in Eqs. (31) and (32); see the diamond-shaped data points in Fig. 1.

Corrections to the result (44) with the $\boldsymbol{\mathcal{E}}^{\rm T\prime}$ term retained were computed analytically by Rädler et al. (2002a,b). The corresponding values are again well reproduced by all flavors of the generalized test-field method as well as by the imposed-field method.

In the first line of Table 2, we repeat the α result for $\tilde{N}_{\rm K} = 1$ and added that for test fields with the wavenumber $k_z = 1$, from where we also come to know the turbulent diffusivity $\eta_{\rm t}$. Note the difference between the values for $k_z = 1$ and $k_z = 0$, which is roughly given by a factor $3/2$ for $k_z = 1$ and $k_{\rm f} = \sqrt{2}$; see Eq. (44). Additionally, the results of the quasi-kinematic method for $k_z = 1$, $\alpha^{\rm QK}$ and $\eta_{\rm t}^{\rm QK}$, are shown. As expected, they coincide completely with α and $\eta_{\rm t}$.

4.1.2. Purely magnetic forcing

Next we consider the case of purely magnetic Roberts forcing, i.e. $N_{\rm K} = 0$. Due to the Beltrami property of $\boldsymbol{f}_{\rm M}$, $\boldsymbol{b}_0 \propto \boldsymbol{f}_{\rm M}$ is also a Beltrami field, so $\boldsymbol{j}_0 \times \boldsymbol{b}_0 = \boldsymbol{0}$ and therefore $\boldsymbol{u}_0 = \boldsymbol{0}$ is a solution of Eqs. (19) and (20). A bifurcation leading to solutions with $\boldsymbol{u}_0 \neq \boldsymbol{0}$ cannot generally be ruled out, but was never observed. Thus we have for the rms value of the magnetic vector potential $a_{0\rm rms} = N_{\rm M}/\eta k_{\rm f}^2$, hence $b_{0\rm rms} = N_{\rm M}/\eta k_{\rm f}$. The appropriate parameter for expressing the strength of the fluctuating magnetic fields is now the Lundquist number and the corresponding analytic result for ${\rm Lu} \ll 1$ reads

$$ \alpha/\alpha_{0\rm M} = ({\rm Lu}/{\rm Pr_M})/[1 + (k_z/k_{\rm f})^2], \quad \alpha_{0\rm M} = 3b_{\rm rms}/4 \tag{45} $$

(for the derivation see Appendix E). It turns out that the sign of α coincides now with that of the helicity of the forcing function.

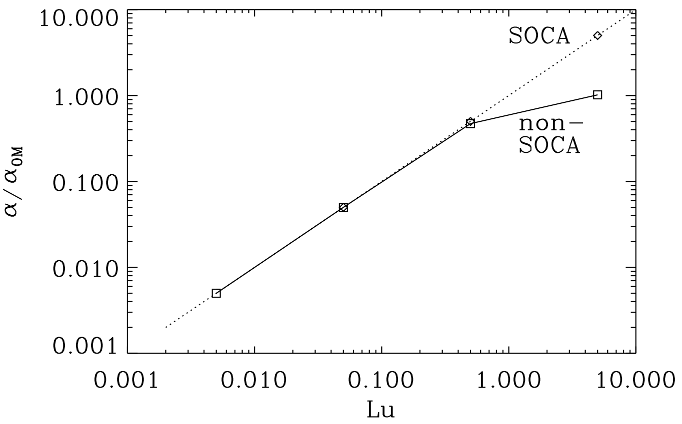

Fig. 2. $\alpha/\alpha_{0\mathrm{M}}$ vs. Lu for purely magnetic Roberts forcing with $k_z = 0$ (2D case) from all versions of the generalized method (solid line with squares). Note the full agreement with Eq. (45) (dotted line) for Lu $\ll$ 1. Diamonds: results of the generalized methods with $\mathcal{F}^{\mathrm{T}\prime}$ and $\mathcal{E}^{\mathrm{T}\prime}$ in Eqs. (31) and (32) neglected, again coinciding with Eq. (45).

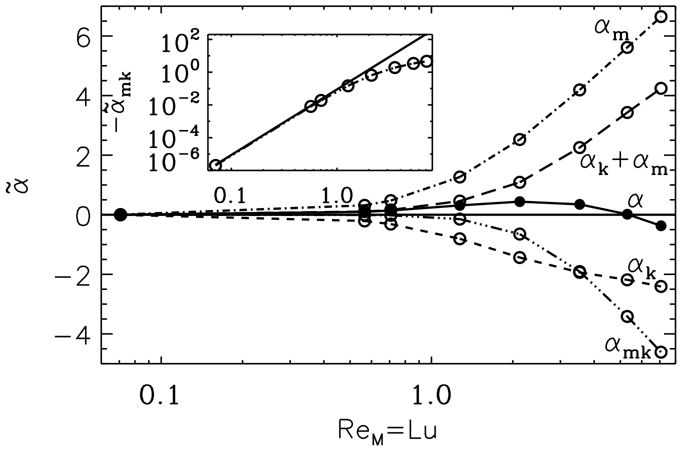

Fig. 3. α versus $\mathrm{Re_M}$ = Lu for hydromagnetic Roberts forcing with $k_z = 0$ (2D case). Along with the total value the constituents α_k, α_m and α_mk as well as $\alpha_\mathrm{k} + \alpha_\mathrm{m}$ are shown. Note the sign change in α at $\mathrm{Re_M} \approx 5.4$. Inset: α_mk in comparison to the result of a fourth order analytical calculation (solid line).

Table 2. Kinematic results for $\tilde{\alpha}$ and $\tilde{\eta}_\mathrm{t}$ for purely hydrodynamic ($\tilde{N}_\mathrm{M} = 0$), purely magnetic ($\tilde{N}_\mathrm{K} = 0$), and hydromagnetic Roberts forcing.

$\tilde{N}_\mathrm{K}$	$\tilde{N}_\mathrm{M}$	$\tilde{\alpha}(k_z = 0)$	$\tilde{\alpha}$	$\tilde{\alpha}^\mathrm{QK}$	$\tilde{\eta}_\mathrm{t}$	$\tilde{\eta}_\mathrm{t}^\mathrm{QK}$
1	0	−0.0857	−0.0569	−0.0569	0.0399	0.0399
0	1	0.2499	0.1684	0.0000	0.1188	0.0000
3.364	0	−0.7330	−0.4734	−0.4734	0.3087	0.3087
0	1.942	0.8219	0.5664	0.0000	0.3983	0.0000
3.364	1.942	−0.0081	0.0664	−0.4734	0.6604	0.3086
3.364	0	−1.0002	−0.6668	−0.6666	0.4715	0.4714[1]
0	1.942	1.0000	0.6666	0.0000	0.4714	0.0000[1]
3.364	1.942	-4×10^{-6}	2×10^{-5}	−0.6666	0.9428	0.4714[1]

Notes. [(1)] With SOCA. Test-field wavenumber $k_z = 1$, except in the third column where $k_z = 0$. These results agree with those of the imposed-field method. $\tilde{\alpha}^\mathrm{QK}$ and $\tilde{\eta}_\mathrm{t}^\mathrm{QK}$ refer to the quasi-kinematic method.

Again, we consider first the two-dimensional case with $k_z = 0$; see Fig. 2. In analogy to purely hydrodynamic forcing we find for Lu $\ll 1$ agreement between all versions of the generalized test-field method (solid line with squares) with Equation (45) (dotted line). For higher values, their SOCA versions (see Sect. 4.1.1) accomplish the same; see diamond data points. Note that for the last data point with Lu = 7 it was necessary to lower the strength of the imposed field to $B_\mathrm{imp}/\eta k_1 = 10^{-4}$, because otherwise the solution of the main run becomes unstable and changes to a new pattern.

The second line of Table 2 repeats the result for $\tilde{N}_\mathrm{M} = 1$, again amended by those for $k_z = 1$ and the results of the quasi-kinematic method, which is obviously unable to produce correct answers. This is because the mean electromotive force is now given by $\boldsymbol{u}_{\overline{B}} \times \boldsymbol{b}_0$, which is only taken into account in the generalized method. Note further that η_t is positive both for hydrodynamic and magnetic forcings.

4.1.3. Hydromagnetic forcing

As already pointed out in Sect. 3.5, in the absence of a mean field, for simultaneous kinetic and magnetic Roberts forcing with $\sigma = 1$ there is a solution of Eqs. (19) and (20) consisting just of the solutions $\boldsymbol{u}_0$ and $\boldsymbol{b}_0$ of the system when forced purely hydrodynamically and magnetically, respectively. Again, a bifurcation leading to another type of solution cannot be ruled out, but was not observed.

In contrast to what one might suppose, however, the decoupling of $\boldsymbol{u}_0$ and $\boldsymbol{b}_0$ lets the value of α for hydromagnetic forcing in general not be simply additive in the values for purely hydrodynamic and purely magnetic forcings. We denote these by $\alpha_\mathrm{k} = \alpha(\boldsymbol{b}_0 = \boldsymbol{0})$ and $\alpha_\mathrm{m} = \alpha(\boldsymbol{u}_0 = \boldsymbol{0})$, respectively. Beyond SOCA[2], the terms $(\boldsymbol{u}_{\overline{B}} \times \boldsymbol{b}_0)'$ and $(\boldsymbol{j}_0 \times \boldsymbol{b}_{\overline{B}} + \boldsymbol{j}_{\overline{B}} \times \boldsymbol{b}_0)'$ in Eqs. (21) and (22) provide couplings between $\boldsymbol{u}_{\overline{B}}$ and $\boldsymbol{b}_{\overline{B}}$ and give rise to an additional "magnetokinetic" part of α, defined as $\alpha_\mathrm{mk} = \alpha - \alpha_\mathrm{k} - \alpha_\mathrm{m}$. Note that we use here lower case subscripts k, m, mk to distinguish this split of the α values from that introduced at the end of Sect. 3.3, which applies only to the nonlinear case. In contrast, the occurrence of α_mk is a purely kinematic effect. While α_k and α_m are, to leading order (and hence in SOCA), quadratic in the respective background fluctuations, the magnetokinetic term is of leading fourth order and is representable in schematic form as $\alpha_\mathrm{mk} \propto \overline{\boldsymbol{u}_0^2\, \boldsymbol{b}_0^2}$.

Lines 5 and 8 of Table 2 show cases with hydromagnetic forcing and amplitudes adjusted such that we would have $\tilde{\alpha}_\mathrm{k} = \tilde{\alpha}_\mathrm{m} = 1$ if SOCA were valid. In either case the preceding two lines present the corresponding purely forced cases. Lines 6 to 8 refer to the SOCA versions of the generalized methods. It can be clearly seen that the results are additive only in the latter case. The value of $\boldsymbol{\alpha}_\mathrm{mk}$ as inferred from lines 3 to 5, is −0.1 resulting in a considerable reduction of α in comparison with the additive value. This is owing to the strong forcing amplitudes, leaving the applicability range of SOCA far behind.

Figure 3 shows α_mk for equally strong velocity and magnetic fluctuations as a function of $\mathrm{Re_M}$ = Lu together with α_k, α_m, $\alpha_\mathrm{k} + \alpha_\mathrm{m}$ and the resulting total value α. Note the significant difference between the naive extrapolation of SOCA, $\alpha_\mathrm{m} + \alpha_\mathrm{k}$, and the true α. In its inset the figure shows the numerical values of α_mk in comparison to the result of a fourth order calculation $\alpha_\mathrm{mk} = -(\sqrt{2}/64)u_\mathrm{rms}^2 b_\mathrm{rms}^2$ (for the derivation see Appendix F).

[2] Note that in the stationary case in addition to $\mathrm{Re_M} \ll 1$ now in general $b_\mathrm{rms}^2 \ll (\nu/l_\mathrm{c})u_\mathrm{rms}$ has to be required for SOCA to be applicable.

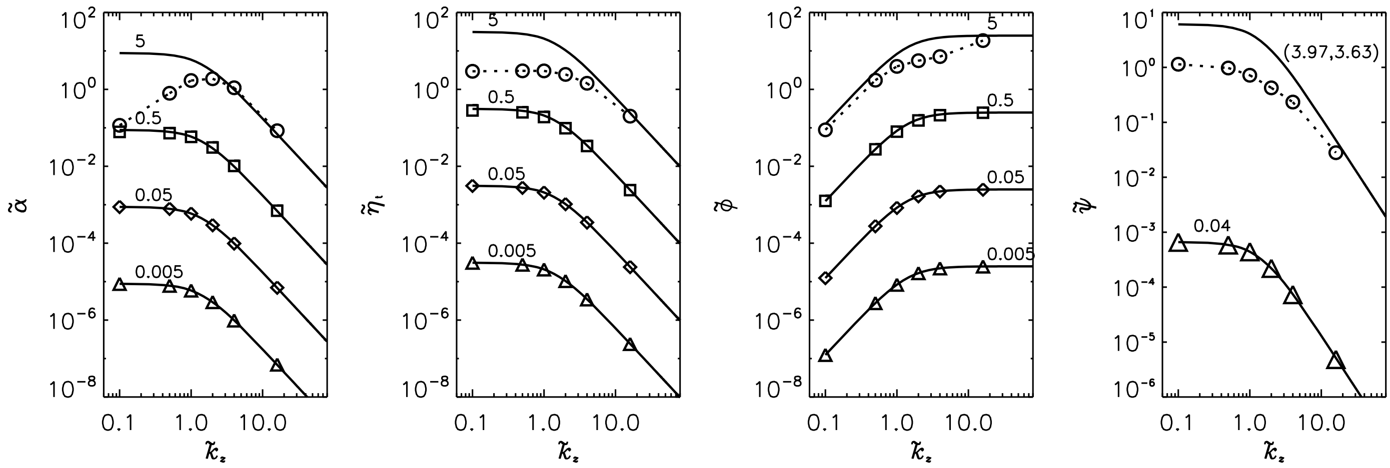

Fig. 4. $\alpha(k_z)$, $\eta_t(k_z)$, and $\phi(k_z)$ for hydromagnetic Roberts forcing with $\sigma = 1$ (*left three panels*), likewise $\psi(k_z)$, but for $\sigma = 0.5$ (*rightmost panel*). Solid lines: SOCA results, cf. Appendix C. Curve labels refer to $\mathrm{Re_M} = \mathrm{Lu}$ or $(\mathrm{Re_M}, \mathrm{Lu})$.

Clearly, the validity range of this expression extends beyond $\mathrm{Re_M} = \mathrm{Lu} = 1$ and hence further than the one of SOCA. It remains to be studied whether the magnetokinetic contribution has a significant effect also in the more general case when $\boldsymbol{u}_0 \not\parallel \boldsymbol{b}_0$. If so, considering α to be the sum of a kinetic and a magnetic part, as often done in quenching considerations, may turn out to be too simplistic.

Likewise one may wonder whether closure approaches to the determination of transport coefficients supposed to be superior to SOCA can be successful at all as long as they do not take fourth order correlations into account properly.

For the tensors $\boldsymbol{\phi}$ and $\boldsymbol{\psi}$, which turn out to show up with simultaneous hydromagnetic and magnetic forcing only (in addition, $\boldsymbol{\phi}$ requires z-dependent mean fields) we have of course again isotropy, $\phi_{11} = \phi_{22} \equiv \phi$, $\psi_{11} = \psi_{22} \equiv \psi$.

As a peculiarity of the Roberts flow, ψ vanishes in the range of validity of SOCA if the helicity is maximum ($\sigma = 1$ in (42)). For this case the first three panels of Fig. 4 show the numerically determined dependences $\alpha(k_z)$, $\eta_t(k_z)$ and $\phi(k_z)$ with different values of $u_{0\mathrm{rms}} = b_{0\mathrm{rms}}$ (data points, dotted lines). The last panel shows $\psi(k_z)$ for $\sigma = 0.5$ and the same forcing amplitudes as before. As explained above, $\boldsymbol{u}_0$ and $\boldsymbol{b}_0$ can now no longer be forced independently from each other. Hence, both fields cannot show exactly the geometry defined by (42) and $u_{0\mathrm{rms}}$ and $b_{0\mathrm{rms}}$ diverge increasingly with increasing forcing.

As demonstrated in Appendix C, $\phi(k_z) \propto k_z^2/(k_z^2 + k_\mathrm{f}^2)$, $\alpha(k_z), \eta_t(k_z), \psi(k_z) \propto 1/(k_z^2 + k_\mathrm{f}^2)$ in the SOCA limit. For comparison these functions are depicted by solid lines. Note the clear deviations from SOCA for $\mathrm{Re_M} = \mathrm{Lu} = 5$, particularly in α. Note also that the expression for ψ was derived under the assumption that the background has the geometry (42). It is therefore not applicable in a strict sense. The clear disagreement with the values of ψ from the test-field method for high values of $\mathrm{Re_M}$ and Lu are hence not only due to violating the SOCA validity constraint.

4.2. Dependence on the mean magnetic field

We now admit dynamically effective mean fields and hence have to deal with anisotropic fluctuating fields $\boldsymbol{u}$ and $\boldsymbol{b}$ which result in anisotropic tensors $\boldsymbol{\alpha}$, $\boldsymbol{\eta}$, $\boldsymbol{\phi}$ and $\boldsymbol{\psi}$. For the chosen forcing, $\overline{\boldsymbol{B}}$ is the only reason for anisotropy in the xy plane, so $\boldsymbol{\alpha}$ has to have the form

$$\alpha_{ij} = \alpha_1 \delta_{ij} + \alpha_2 \hat{B}_i \hat{B}_j, \quad i, j = 1, 2,$$

with $\hat{\boldsymbol{B}}$ being the unit vector in the direction of $\overline{\boldsymbol{B}}$ (here the x direction). We obtain then $\alpha_{11} = \alpha_1 + \alpha_2$ and $\alpha_{22} = \alpha_1$. Of course, the tensors $\boldsymbol{\eta}$, $\boldsymbol{\phi}$ and $\boldsymbol{\psi}$ are built analogously. Clearly, irrespective of whether the forcing is pure or mixed, the effects of B_imp prevent $\boldsymbol{u}$ and $\boldsymbol{b}$ from having Roberts geometry.

In general, we leave in this section safe mathematical grounds and enter empirical work. Only for vanishing magnetic background, $\boldsymbol{b}_0 = \boldsymbol{0}$, one version of the generalized method does coincide with the quasi-kinematic one (see Sect. 3.4, Remark (iii)) and will therefore guarantee correct results.

4.2.1. Purely hydrodynamic forcing

In this case we have $\overline{\boldsymbol{\mathcal{E}}}_{\bar{B}} = \overline{\boldsymbol{u} \times \boldsymbol{b}_{\bar{B}}} = \overline{\boldsymbol{\mathcal{E}}}{}^\mathrm{K}_{\bar{B}}$ and all flavors of the generalized method have to yield results which coincide with those of the quasi-kinematic method. This is valid to very high accuracy for the ju and bu versions and somewhat less perfectly so for the bb and jb versions. We emphasize that the presence of B_imp, being solely responsible for the occurrence of magnetic fluctuations, does not result in a failure of the quasi-kinematic method as one might conclude from the model used by Courvoisier et al. (2010).

Figure 5 presents the constituents of $\boldsymbol{\alpha}$ as functions of the imposed field in the 2D case. We may conclude from the data that α_2 is negative and approximately equal to α_{11}^M. For values of $B_\mathrm{imp}/\eta k_1 > 5$, its modulus approaches $\alpha_{22} = \alpha_1$ and thus gives rise to the strong quenching of the effective $\alpha = \alpha_{11}$. Indeed, $\alpha(B_\mathrm{imp})$ can be described by a power law with an exponent -4 for large B_imp. This is at odds with analytic results predicting either $\alpha \propto B^{-2}$ (Field et al. 1999; Rogachevskii & Kleeorin 2000) or $\propto B^{-3}$ (Moffatt 1972; Rüdiger 1974). By comparing with computations in which the non-SOCA term was neglected, we have checked that our discrepancy with these predictions is not a consequence of SOCA applied therein. Sur et al. (2007) suggested that the B^{-2} and B^{-3} dependence is likely to be valid for time-dependent and steady flows, respectively. It should be noted, however, that their numerical values for the steady ABC flow do actually exhibit the B^{-4} power law; cf. their Fig. 2. They also found that an α^M, defined similarly to our α_{11}, increases

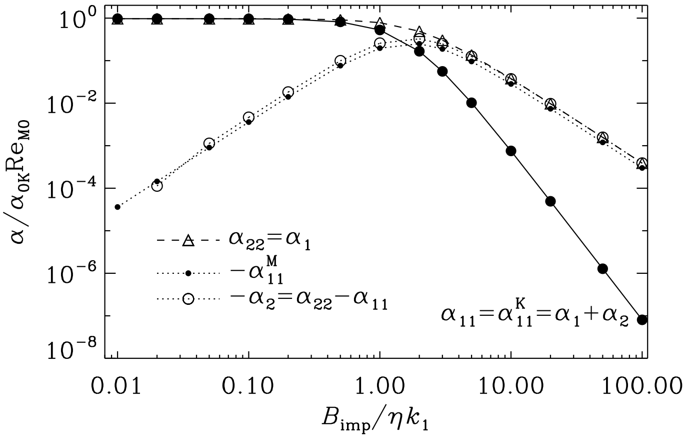

Fig. 5. α_{11} (solid line, filled circles) and α_{22} (dashed line, open triangles) as functions of the imposed field strength B_{imp}, compared with $-\alpha_{11}^M$ (dotted line, small dots) and $\alpha_{22}-\alpha_{11}=-\alpha_2$ (dotted line, open circles) for purely kinetic Roberts forcing with $\tilde{N}_K = 1$. $\alpha_{11}^M \approx \alpha_2$ throughout. Note that $\alpha_{0K} < 0$ and that the α symbols in the legend refer to quantities that are normalized by $\alpha_{0K}\mathrm{Re}_{M0}$ and hence sign-inverted.

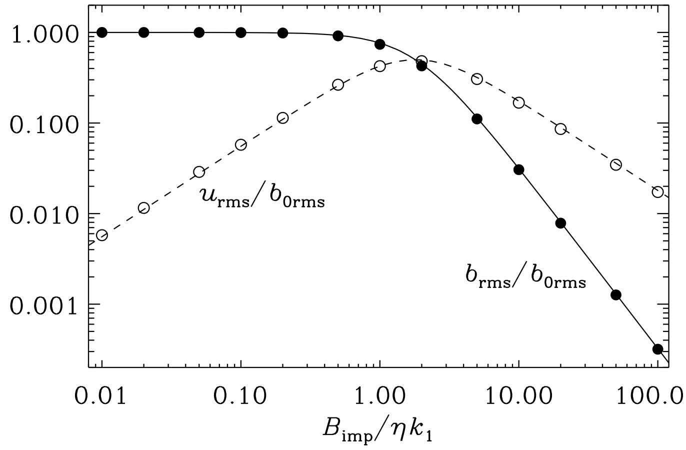

Fig. 6. Root-mean-square values u_{rms} (open circles) and b_{rms} (filled circles) as functions of the imposed field strength B_{imp} for purely magnetic Roberts forcing, $\tilde{N}_M = 1$. Solid and dashed lines represent the fits given by Eq. (46).

quadratically with $\overline{\boldsymbol{B}}$ for weak fields and declines quadratically for strong fields. This is in agreement with our present results.

4.2.2. Purely magnetic forcing

Here, the mean electromotive force is simply $\overline{\boldsymbol{\mathcal{E}}} = \overline{\boldsymbol{\mathcal{E}}}^M_{\overline{B}} = \overline{\boldsymbol{u}_{\overline{B}} \times \boldsymbol{b}}$. This is true as long as significant velocities in the main run occur only due to the presence of the mean field, that is, as long as $\boldsymbol{u}_0 = \boldsymbol{0}$ (see above). While $\overline{\boldsymbol{B}}$ is weak, $\overline{\boldsymbol{\mathcal{E}}}$ is approximately $\overline{\boldsymbol{u}_{\overline{B}} \times \boldsymbol{b}_0}$. However, one could speculate that, if the imposed field reaches appreciable levels, i.e., if $\boldsymbol{u}$ is sufficiently strong, $\overline{\boldsymbol{\mathcal{E}}}$ can with good accuracy be approximated by $\overline{\boldsymbol{\mathcal{E}}}^K_{\overline{B}} = \overline{\boldsymbol{u} \times \boldsymbol{b}_{\overline{B}}}$. Since the quasi-kinematic method takes just this term into account, it could then produce useful results.

In Fig. 6 we show the rms values of the resulting velocity and magnetic fields as functions of the imposed field strength for $\tilde{N}_M = 1$, corresponding to Lu $= 1/2$ if $\boldsymbol{B}_{imp} = \boldsymbol{0}$. The data points can be fitted by expressions of the form

$$\frac{b_{rms}}{b_{0rms}} = \frac{1}{1 + B_{imp}^2/B_*^2}, \quad \frac{u_{rms}}{b_{0rms}} = \frac{B_{imp}/B_*}{1 + B_{imp}^2/B_*^2}, \qquad (46)$$

where $B_*/\eta k_1 \approx 1.8\,\tilde{N}_M$. Note, that indeed the velocity fluctuations become dominant over the magnetic ones for $B_{imp}/\eta k_1 > 2$.

The resulting finding, as shown in Fig. 7, is completely analogous to the one of Sect. 4.2.1, but now we see $-\alpha_{11}^K \approx -\alpha_2$ approaching $\alpha_{22} = \alpha_1$ with increasing B_{imp}. Hence, the idea that the quasi-kinematic method could give reasonable results for strong mean fields has not proven true as α_{11}^K is not approaching α_{11}, despite the domination of u_{rms} over b_{rms}. Instead, the values from the quasi-kinematic method have the wrong sign and deviate in their moduli by several orders of magnitude.

In Table 3 we compare, for different values of B_{imp}, the values of α_{11} and α_{22}, obtained using the generalized test-field method, with those of α_{11}^K and those from the quasi-kinematic method, α_{11}^{QK} and α_{22}^{QK}, where the entire dynamics of $\boldsymbol{u}_{\overline{B}}$ has been ignored. Note again, that the results of all four versions of the generalized test-field method agree with each other.

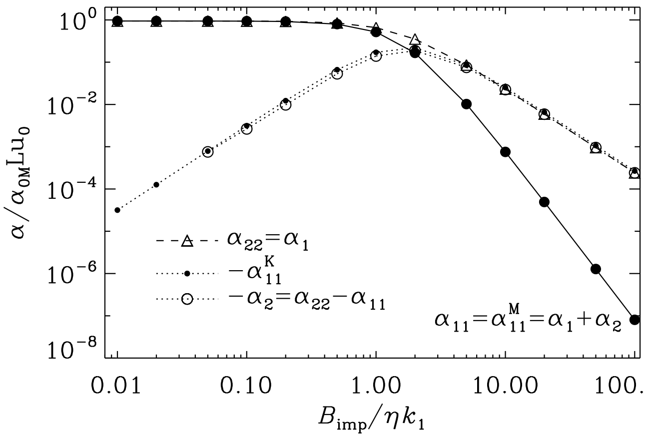

Fig. 7. α_{11} (solid line, filled circles) and α_{22} (dashed line, open triangles) as functions of the imposed field strength B_{imp}, compared with $-\alpha_{11}^K$ (dotted line, small dots) and $\alpha_{22}-\alpha_{11}=-\alpha_2$ (dotted line, open circles) for purely magnetic Roberts forcing with $\tilde{N}_M = 1$. Note that $\alpha_{11}^K \approx \alpha_2$ throughout.

Table 3. Dependence of $\tilde{\alpha}_{11}$ and $\tilde{\alpha}_{22}$ from the generalized method on $\tilde{B}_{imp}$ for $\tilde{N}_K = 0$ and $\tilde{N}_M = 1$ together with the kinetic contribution $\tilde{\alpha}_{11}^K$ and the results from the quasi-kinematic method ($\tilde{\alpha}_{11}^{QK}$ and $\tilde{\alpha}_{22}^{QK}$).

$\tilde{B}_{imp}$	10^{-2}	1	10^1	10^2
$\tilde{\alpha}_{11}$	2.499×10^{-1}	1.376×10^{-1}	2.000×10^{-4}	2.131×10^{-8}
$\tilde{\alpha}_{22}$	2.499×10^{-1}	1.747×10^{-1}	6.161×10^{-3}	6.390×10^{-5}
$\tilde{\alpha}_{11}^K$	-8.391×10^{-6}	-4.540×10^{-2}	-6.666×10^{-3}	-7.067×10^{-5}
$\tilde{\alpha}_{11}^{QK}$	-7.858×10^{-6}	-4.350×10^{-2}	-6.657×10^{-3}	-7.067×10^{-5}
$\tilde{\alpha}_{22}^{QK}$	-2.247×10^{-7}	-1.152×10^{-3}	-4.740×10^{-7}	-5.326×10^{-13}

4.2.3. Hydromagnetic forcing

In analogy to Figs. 5 and 7 we show in Fig. 8 the constituents of $\boldsymbol{\alpha}$ versus B_{imp}. Note that we have used here $\alpha_{0K}\mathrm{Re}_{M0} + \alpha_{0M}\mathrm{Lu}_0 > 0$ for normalizing $\boldsymbol{\alpha}$. This is the kinematic value of $\alpha_{11} = \alpha_{22}$ for $k_z = 0$ and small u_{0rms}, b_{0rms}; see Eqs. (44), (45) and Sect. 4.1.3.

It can be observed that α_{11}^M at first dominates over $-\alpha_{11}^K$, but at $B_{imp}/\eta k_1 \approx 2$ their relation reverses. Remarkably, the ratio of

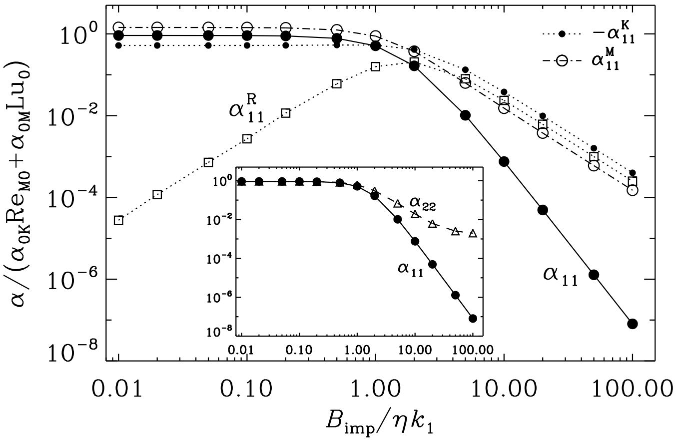

Fig. 8. α_{11} (solid line, filled circles) as function of the imposed field strength B_{imp}, compared with $-\alpha_{11}^{K}$ (dotted line, small dots), α_{11}^{M} (dash-dotted line, open circles) and α_{11}^{R} (dotted line, open squares) for hydromagnetic Roberts forcing with $\tilde{N}_M = \tilde{N}_K = 1$. Inset: α_{22} (dashed line, open triangles) compared to α_{11}.

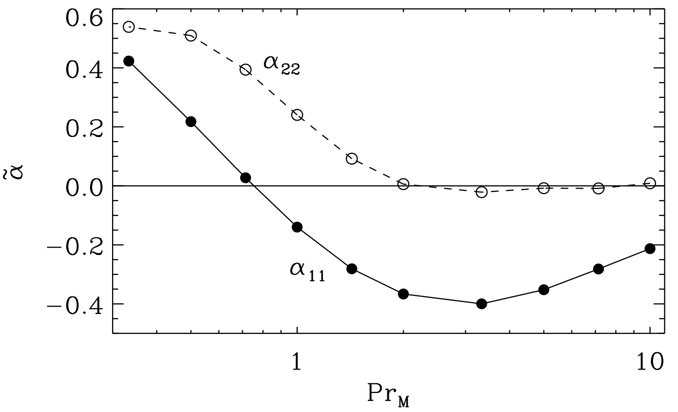

Fig. 9. Dependence of α_{11} and α_{22} on Pr_M for hydromagnetic Roberts forcing with $\mathrm{Lu}/\mathrm{Re}_M = 1$ and $B_{imp}/\nu k_1 = 1$.

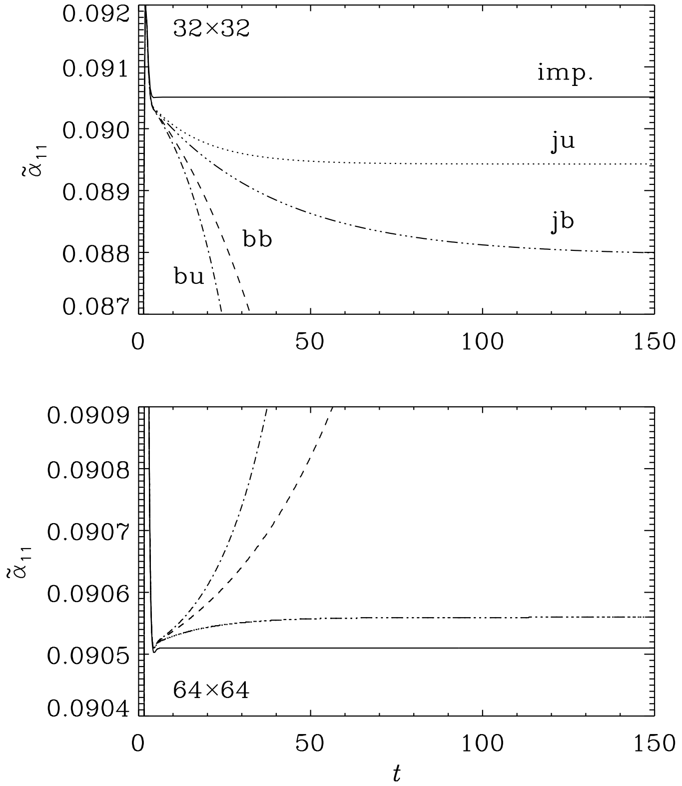

Fig. 10. Convergence of α_{11} from the ju and jb versions of the generalized method to the result of the imposed-field method and exponential divergence of the versions bu and bb for $\widetilde{N}_K = \widetilde{N}_M = 1$, $\tilde{B}_{imp} = 1$, $k_z = 0$ and a resolution of either 32^2 (*upper panel*) or 64^2 mesh points (*lower panel*). Note the improving agreement between the ju and jb versions: the deviation is changing from ≈2.5% to ≈0.05%, that is, by a factor $\approx 2^6$, as expected for a sixth order finite difference scheme.

their moduli reaches, for high values of B_{imp}, just the inverse of that for low values. The strong quenching of α_{11} is now a consequence of α_{11}^{R} approaching $-\alpha_{11}^{K} - \alpha_{11}^{M}$. In complete agreement with the former two cases with pure forcings, $-\alpha_{11}$ is proportional to B_{imp}^{-4} for strong fields. However, we see a deviating behavior of $\alpha_{22}(B_{imp})$ as it is no longer following a power law.

Given that the α effect can be sensitive to the value of Pr_M, we study α_{11} and α_{22} as functions of Pr_M, keeping $\mathrm{Lu}/\mathrm{Re}_M = 1$ and $B_{imp}/\nu k_1 = 1$ fixed. The result is shown in Fig. 9. In the interval $0.3 \le \mathrm{Pr}_M \le 2$, the α coefficients exhibit a high sensitivity with respect to Pr_M changing even their sign at $\mathrm{Pr}_M \approx 0.7$ and 2, respectively. Note also the occurrence of minima.

4.3. Convergence

In most of the cases the four different versions of the generalized method (see Table 1) give quite similar results. For purely hydrodynamic and purely magnetic forcing there is agreement to all significant digits. This is not quite so perfect with hydromagnetic forcing, i.e. $N_K \neq 0$, $N_M \neq 0$. In general, however, agreement is improved by increasing the numerical resolution.

Yet another complication arises when $B_0 \neq 0$, because then some of the versions are found to display exponentially growing test solutions; see Fig. 10. This may not be surprising, because each version corresponds to a different linear inhomogeneous system of equations, and there is no guarantee that each of them has only stable solutions. The actual occurrence of instabilities depends however on intricate properties of the fluctuating fields from the main run, $\boldsymbol{u}$ and $\boldsymbol{b}$. We suppose that, if one could remove the unstable eigenvalues of the homogeneous part of the system (31)–(34) from its spectrum, the solution of the inhomogeneous system would indeed be the correct one.

5. Discussion

The main purpose of the developed method consists in handling situations in which hydrodynamic and magnetic fluctuations coexist in the background. The quasi-kinematic method can only afford those constituents of the mean-field coefficients that are related solely to the hydrodynamic background $\boldsymbol{u}_0$, but the new method is capable of delivering, in addition, those related to the magnetic background $\boldsymbol{b}_0$. Moreover, it is able to detect mean-field effects that depend on cross correlations of $\boldsymbol{u}_0$ and $\boldsymbol{b}_0$. We have demonstrated this with the two fluctuations being forced externally to have the same Roberts-like geometry. With respect to α we observe a “magneto-kinetic” part being, to leading order, quadratic in the magnetic Reynolds and Lundquist numbers. It is capable of reducing the total α significantly in comparison with the sum of the α values resulting from purely hydrodynamic and purely magnetic backgrounds. In contrast, the tensors $\boldsymbol{\phi}$ and $\boldsymbol{\psi}$ which give rise to the occurrence of mean forces proportional to $\nabla(\nabla\overline{\boldsymbol{B}})$ and $\nabla\overline{\boldsymbol{B}}$ are, to leading order, bilinear in $\mathrm{Re_M}$ and Lu.

In nature, however, external electromotive forces imprinting finite cross-correlations of $\boldsymbol{u}_0$ and $\boldsymbol{b}_0$ are rarely found. Therefore the question regarding the astrophysical relevance of these effects has to be posed. Given the high values of $\mathrm{Re_M}$ in practically all cosmic bodies, small-scale dynamos are supposed to be ubiquitous and do indeed provide hydromagnetic background turbulence. But is it realistic to expect non-vanishing cross-correlations under these circumstances?

Let us consider a number of similar, yet not completely identical turbulence cells arranged in a more or less regular pattern. As dynamo fields are solutions of the homogeneous induction equation and the Lorentz force is quadratic in $\boldsymbol{B}$, bilinear cross-correlations, $\overline{u_{0i}b_{0j}}$, obtained by averaging over single cells can be expected to change their sign randomly from cell to cell provided the cellular dynamos have evolved independently from each other. Consequently, the average over many cells would approach zero and the $\boldsymbol{\phi}$ and $\boldsymbol{\psi}$ effects would not occur. In contrast, cross-correlations that are even functions of the components of $\boldsymbol{b}_0$ and their derivatives, were not rendered zero due to random polarity changes in the small-scale dynamo fields (e.g. the magneto-kinetic α).

However, the assumption of independently acting cellular dynamos can be put in question when the whole process beginning with the onset of the turbulence-creating instability (e.g. convection) is taken into account. During its early stages, i.e. for small magnetic Reynolds numbers, the flow is at first unable to allow for any dynamo action, but with growing amplitude a large-scale dynamo can be excited first to create a field that is coherent over many turbulence cells. With further growth of its amplitude the (hydrodynamic) turbulence eventually enters a stage in which small-scale dynamo action becomes possible. The seed fields for these dynamos are now prevailingly determined by the already existing mean field and due to its spatial coherence the polarity of the small-scale field is not settling independently from cell to cell, thus potentially allowing for non-vanishing cross-correlations. Moreover, instead of employing the idea of a pre-existing large-scale dynamo one may claim that, given the smallness of the turbulence cells compared to the scale of the surroundings of the cosmic object, there is always a large-scale field, e.g. the galactic one, that is coherent across a large number of turbulence cells.

But even if one wants to abstain from employing the influence of a pre-existing mean field it has to be considered that neighboring cells are never exactly equal. Thus, in the course of the growing amplitude of the hydrodynamic background, in some of them the small-scale dynamo will start working first, hence setting the seed field for its immediate neighbors. It is well conceivable that a certain sign of, say, the cross-correlation, $\overline{u_{0i}b_{0j}}$, established in one of the early starting cells "cascades" to more and more distant neighbors until this process is limited by the cascades originating from other early starting cells. Consequently, we arrive at a situation similar to the one discussed before, yet with less extended regions of coinciding signs of the correlation.

In summary, cross-correlations and the mean-field effects connected to them cannot be ruled out a priori. Direct numerical simulations of the scenarios discussed above should be performed in order to clarify the significance of these effects. This is equally valid for the effects due to cross-correlations resulting in $\overline{\boldsymbol{\mathcal{E}}}_0$; see Eq. (28).

In a recent paper, Courvoisier et al. (2010) discuss the range of applicability of the quasi-kinematic test-field method. Their model consists of the equations of incompressible magnetohydrodynamics with purely hydrodynamic forcing. However, by imposing an additional uniform magnetic field $\boldsymbol{\mathcal{B}}$ together with the forced fluctuating velocity a fluctuating magnetic field arises. It must be stressed that, following the line of their argument, these fluctuations have to be considered as part of the *background* $(\boldsymbol{u}_0, \boldsymbol{b}_0)$, that is, they belong to those fluctuations that occur in the *absence* of the mean field. This follows from the fact that, when defining transport coefficients such as $\boldsymbol{\alpha}$, the field $\boldsymbol{\mathcal{B}}$ is not regarded as part of the mean field $\overline{\boldsymbol{B}}$, in contrast to our treatment; see their Sect. 2b. For simplicity they consider only the kinematic case and restrict the analysis to mean fields $\propto e^{ik_z z}$ with $k_z \to 0$. In their main conclusion, drawn under these conditions, they state that the quasi-kinematic test-field method, which considers only the magnetic response to a mean magnetic field, must fail for $\boldsymbol{\mathcal{B}} \neq \boldsymbol{0}$, that is $\boldsymbol{b}_0 \neq \boldsymbol{0}$. We fully agree in this respect, but should point out that the quasi-kinematic method was not claimed to be applicable in that case; see Brandenburg et al. (2008c, Sect. 3) giving the caveat "As in almost all supercritical runs a small-scale dynamo is operative, our results which are derived under the assumption of its influence being negligible may contain a systematic error.". However, Courvoisier et al. (2010) overinterpret their finding in postulating that already the determination of quenched coefficients such as $\alpha(\overline{B})$ for $\boldsymbol{b}_0 = \boldsymbol{0}$ by means of the quasi-kinematic method leads to wrong results. The paper of Tilgner & Brandenburg (2008), quoted by them in this context, is just proving evidence for the correctness of the method, as does Brandenburg et al. (2008c).

Our tensor $\boldsymbol{\psi}$ is related to their newly introduced mean-field coefficient $\boldsymbol{\Gamma}$ by $\psi_{ij} = \epsilon_{kj3}\Gamma_{i3k}$. Unfortunately, an attempt to reproduce their results for $\boldsymbol{\Gamma}$ (and likewise for $\boldsymbol{\alpha}$) is not currently possible owing to our modified hydrodynamics. We postpone this task to a future paper.

6. Conclusions

Having been applied to situations with a magnetohydrodynamic background where both $\boldsymbol{u}_0$ and $\boldsymbol{b}_0$ have Roberts geometry, the proposed method has proven its potential for determining turbulent transport coefficients. In particular, effects connected with cross-correlations between $\boldsymbol{u}_0$ and $\boldsymbol{b}_0$ have been identified and were found to be in full agreement with analytical predictions as far as they are available. No basic restrictions with respect to the magnetic Reynolds number or the strength of the mean field, which causes the nonlinearity of the problem, are observed so far. As a next step, of course, the simplifications in the hydrodynamics used here have to be dropped, thus allowing to produce more relevant results and facilitating comparison with work already done.

Due to the fact that we have no strict mathematical proof for its correctness, there can be no full certainty about the general reliability of the method. An encouraging hint is given by the fact that all four flavors of the method produce often nearly identical results. Occasionally, however, some of them show unstable behavior in the test solutions. Clearly, further exploration of the method's degree of reliance is necessary by including three-dimensional and time-dependent backgrounds. Homogeneity should be abandoned and backgrounds which come closer to real turbulence such as forced turbulence or turbulent convection in a layer are to be taken into account.

Thus, the utilized approach of establishing a test-field procedure in a situation where the governing equations are inherently nonlinear (although by virtue of the Lorentz force only) has proven to be promising. This fact encourages us to develop test-field methods for determining turbulent transport coefficients connected with similar nonlinearities in the momentum equation. An interesting target is the turbulent kinematic viscosity tensor and especially its off-diagonal components that can give rise to a mean-field vorticity dynamo (Elperin et al. 2007; Käpylä et al. 2009), as well as the so-called anisotropic kinematic α effect (Frisch et al. 1987; Sulem et al. 1989; Brandenburg & von Rekowski 2001; Courvoisier et al. 2010) and the Λ effect (Rüdiger 1980, 1982). Yet another example is given by the turbulent transport coefficients describing effective magnetic pressure and tension forces due to the quadratic dependence of the total Reynolds stress tensor on the mean magnetic field (e.g., Rogachevskii & Kleeorin 2007; Brandenburg et al. 2010).

Acknowledgements. We thank Kandaswamy Subramanian for insightful comments that have improved the presentation of our work. This work was supported in part by the European Research Council under the AstroDyn Research Project No. 227952 and the Swedish Research Council Grant No. 621-2007-4064.

Appendix A: Incompressibility

The equations used in this paper have the advantage of simplifying the derivation of the generalized test-field method, but the resulting flows are not realistic because the pressure and advective terms are absent. Here we drop these restrictions and derive the test equations in the incompressible case with constant density. The full momentum and induction equations take then the form

$$\frac{\partial \boldsymbol{U}}{\partial t} = \boldsymbol{U}\times\boldsymbol{W} + \boldsymbol{J}\times\boldsymbol{B} + \boldsymbol{F}_{\rm K} + \nu\nabla^2\boldsymbol{U} - \boldsymbol{\nabla}P, \tag{A.1}$$

$$\frac{\partial \boldsymbol{A}}{\partial t} = \boldsymbol{U}\times\boldsymbol{B} + \boldsymbol{F}_{\rm M} + \eta\nabla^2\boldsymbol{A}, \tag{A.2}$$

where $\boldsymbol{W} = {\rm curl}\,\boldsymbol{U}$ is the vorticity. P is the sum of gas and dynamical pressure and absorbs the constant density. The corresponding mean-field equations are

$$\frac{\partial \overline{\boldsymbol{U}}}{\partial t} = \overline{\boldsymbol{U}}\times\overline{\boldsymbol{W}} + \overline{\boldsymbol{J}}\times\overline{\boldsymbol{B}} + \overline{\boldsymbol{\mathcal{F}}} + \nu\nabla^2\overline{\boldsymbol{U}} - \boldsymbol{\nabla}\overline{P}, \tag{A.3}$$

$$\frac{\partial \overline{\boldsymbol{A}}}{\partial t} = \overline{\boldsymbol{U}}\times\overline{\boldsymbol{B}} + \overline{\boldsymbol{\mathcal{E}}} + \eta\nabla^2\overline{\boldsymbol{A}}, \tag{A.4}$$

where $\overline{\boldsymbol{\mathcal{F}}} = \overline{\boldsymbol{u}\times\boldsymbol{w}} + \overline{\boldsymbol{j}\times\boldsymbol{b}}$ and $\overline{\boldsymbol{\mathcal{E}}} = \overline{\boldsymbol{u}\times\boldsymbol{b}}$, and the forcings were assumed to vanish on averaging. The equations for the fluctuations are consequently

$$\frac{\partial \boldsymbol{u}}{\partial t} = \overline{\boldsymbol{U}}\times\boldsymbol{w} + \boldsymbol{u}\times\overline{\boldsymbol{W}} + \overline{\boldsymbol{J}}\times\boldsymbol{b} + \boldsymbol{j}\times\overline{\boldsymbol{B}} + \boldsymbol{\mathcal{F}}' + \boldsymbol{F}_{\rm K} + \nu\nabla^2\boldsymbol{u} - \boldsymbol{\nabla}p, \tag{A.5}$$

$$\frac{\partial \boldsymbol{a}}{\partial t} = \overline{\boldsymbol{U}}\times\boldsymbol{b} + \boldsymbol{u}\times\overline{\boldsymbol{B}} + \boldsymbol{\mathcal{E}}' + \boldsymbol{F}_{\rm M} + \eta\nabla^2\boldsymbol{a}, \tag{A.6}$$

where $\boldsymbol{\mathcal{F}}' = (\boldsymbol{u}\times\boldsymbol{w} + \boldsymbol{j}\times\boldsymbol{b})'$ and $\boldsymbol{\mathcal{E}}' = (\boldsymbol{u}\times\boldsymbol{b})'$. As above we split the fields and likewise Eqs. (A.5) and (A.6) into two parts, i.e. we write $\boldsymbol{u} = \boldsymbol{u}_0 + \boldsymbol{u}_{\overline{B}}$ and $\boldsymbol{a} = \boldsymbol{a}_0 + \boldsymbol{a}_{\overline{B}}$ and arrive at

$$\frac{\partial \boldsymbol{u}_0}{\partial t} = \overline{\boldsymbol{U}}\times\boldsymbol{w}_0 + \boldsymbol{u}_0\times\overline{\boldsymbol{W}} + \boldsymbol{\mathcal{F}}_0' + \boldsymbol{F}_{\rm K} + \nu\nabla^2\boldsymbol{u}_0 - \boldsymbol{\nabla}p_0, \tag{A.7}$$

$$\frac{\partial \boldsymbol{a}_0}{\partial t} = \overline{\boldsymbol{U}}\times\boldsymbol{b}_0 + \boldsymbol{\mathcal{E}}_0' + \boldsymbol{F}_{\rm M} + \eta\nabla^2\boldsymbol{a}_0, \tag{A.8}$$

and the equations for the $\overline{\boldsymbol{B}}$ dependent parts

$$\frac{\partial \boldsymbol{u}_{\overline{B}}}{\partial t} = \overline{\boldsymbol{U}}\times\boldsymbol{w}_{\overline{B}} + \boldsymbol{u}_{\overline{B}}\times\overline{\boldsymbol{W}} + \overline{\boldsymbol{J}}\times\boldsymbol{b} + \boldsymbol{j}\times\overline{\boldsymbol{B}} + \boldsymbol{\mathcal{F}}_{\overline{B}}' + \nu\nabla^2\boldsymbol{u}_{\overline{B}} - \boldsymbol{\nabla}p_{\overline{B}}, \tag{A.9}$$

$$\frac{\partial \boldsymbol{a}_{\overline{B}}}{\partial t} = \overline{\boldsymbol{U}}\times\boldsymbol{b}_{\overline{B}} + \boldsymbol{u}\times\overline{\boldsymbol{B}} + \boldsymbol{\mathcal{E}}_{\overline{B}}' + \eta\nabla^2\boldsymbol{a}_{\overline{B}}, \tag{A.10}$$

where $\boldsymbol{\mathcal{F}}' = \boldsymbol{\mathcal{F}}_0' + \boldsymbol{\mathcal{F}}_{\overline{B}}'$ and $\boldsymbol{\mathcal{E}}' = \boldsymbol{\mathcal{E}}_0' + \boldsymbol{\mathcal{E}}_{\overline{B}}'$ with $\boldsymbol{\mathcal{F}}_0' = (\boldsymbol{u}_0\times\boldsymbol{w}_0 + \boldsymbol{j}_0\times\boldsymbol{b}_0)'$, $\boldsymbol{\mathcal{E}}_0' = (\boldsymbol{u}_0\times\boldsymbol{b}_0)'$, and

$$\boldsymbol{\mathcal{F}}_{\overline{B}}' = (\boldsymbol{j}_0\times\boldsymbol{b}_{\overline{B}} + \boldsymbol{j}_{\overline{B}}\times\boldsymbol{b}_0 + \boldsymbol{j}_{\overline{B}}\times\boldsymbol{b}_{\overline{B}} + \boldsymbol{u}_0\times\boldsymbol{w}_{\overline{B}} + \boldsymbol{u}_{\overline{B}}\times\boldsymbol{w}_0 + \boldsymbol{u}_{\overline{B}}\times\boldsymbol{w}_{\overline{B}})', \tag{A.11}$$

$$\boldsymbol{\mathcal{E}}_{\overline{B}}' = (\boldsymbol{u}_0\times\boldsymbol{b}_{\overline{B}} + \boldsymbol{u}_{\overline{B}}\times\boldsymbol{b}_0 + \boldsymbol{u}_{\overline{B}}\times\boldsymbol{b}_{\overline{B}})'. \tag{A.12}$$

We can rewrite these equations such that they become formally linear in $\boldsymbol{u}_{\overline{B}}$ and $\boldsymbol{b}_{\overline{B}}$. Following the pattern utilized in Sect. 3.3 we find already for $\boldsymbol{\mathcal{F}}_{\overline{B}}'$ four different ways of doing that. Together with the two variants in the case of $\boldsymbol{\mathcal{E}}_{\overline{B}}'$ we finally obtain eight flavors of the test-field method where again in either case $\overline{\boldsymbol{\mathcal{F}}}_{\overline{B}}$ and $\overline{\boldsymbol{\mathcal{E}}}_{\overline{B}}$ are to be constructed analogously to $\boldsymbol{\mathcal{F}}_{\overline{B}}'$ and $\boldsymbol{\mathcal{E}}_{\overline{B}}'$. One of these flavors is defined by

$$\boldsymbol{\mathcal{F}}_{\overline{B}}' = (\boldsymbol{u}\times\boldsymbol{w}_{\overline{B}} + \boldsymbol{u}_{\overline{B}}\times\boldsymbol{w}_0 + \boldsymbol{j}\times\boldsymbol{b}_{\overline{B}} + \boldsymbol{j}_{\overline{B}}\times\boldsymbol{b}_0)', \tag{A.13}$$

$$\boldsymbol{\mathcal{E}}_{\overline{B}}' = (\boldsymbol{u}\times\boldsymbol{b}_{\overline{B}} + \boldsymbol{u}_{\overline{B}}\times\boldsymbol{b}_0)'. \tag{A.14}$$

It is the one which comes closest to the quasi-kinematic test-field method, because there $\boldsymbol{\mathcal{E}}_{\overline{B}}' = (\boldsymbol{u}\times\boldsymbol{b}_{\overline{B}})'$. Next, we substitute $\overline{\boldsymbol{B}}$ by a test field, $\overline{\boldsymbol{B}}^{\rm T}$, and $\boldsymbol{u}_{\overline{B}}$ and $\boldsymbol{b}_{\overline{B}}$ by the test solutions, $\boldsymbol{u}^{\rm T}$ and $\boldsymbol{b}^{\rm T}$, i.e.

$$\frac{\partial \boldsymbol{u}^{\rm T}}{\partial t} = \overline{\boldsymbol{U}}\times\boldsymbol{w}^{\rm T} + \boldsymbol{u}^{\rm T}\times\overline{\boldsymbol{W}} + \overline{\boldsymbol{J}}^{\rm T}\times\boldsymbol{b} + \boldsymbol{j}\times\overline{\boldsymbol{B}}^{\rm T} + \boldsymbol{\mathcal{F}}^{\rm T\prime} + \nu\nabla^2\boldsymbol{u}^{\rm T} - \boldsymbol{\nabla}p^{\rm T}, \tag{A.15}$$

$$\frac{\partial \boldsymbol{a}^{\rm T}}{\partial t} = \overline{\boldsymbol{U}}\times\boldsymbol{b}^{\rm T} + \boldsymbol{u}\times\overline{\boldsymbol{B}}^{T} + \boldsymbol{\mathcal{E}}^{\rm T\prime} + \eta\nabla^2\boldsymbol{a}^{\rm T}, \tag{A.16}$$

where

$$\boldsymbol{\mathcal{F}}^{\rm T\prime} = (\boldsymbol{u}\times\boldsymbol{w}^{\rm T} + \boldsymbol{u}^{\rm T}\times\boldsymbol{w}_0 + \boldsymbol{j}\times\boldsymbol{b}^{\rm T} + \boldsymbol{j}^{\rm T}\times\boldsymbol{b}_0)', \tag{A.17}$$

$$\boldsymbol{\mathcal{E}}^{\rm T\prime} = (\boldsymbol{u}\times\boldsymbol{b}^{\rm T} + \boldsymbol{u}^{\rm T}\times\boldsymbol{b}_0)'. \tag{A.18}$$

For the mean electromotive and ponderomotive force the ansatzes Eqs. (7) and (15) can be employed without change. Note, however, that the tensors $\boldsymbol{\phi}$ and $\boldsymbol{\psi}$ now contain contributions from the Reynolds stress caused by $\boldsymbol{u}_{\overline{B}}$, that is, eventually by $\overline{\boldsymbol{B}}$.

Appendix B: Completeness of ansatzes (7) and (15)

The ansatzes Eqs. (7) and (15) are not exhaustive because higher spatial and all temporal derivatives of $\overline{\boldsymbol{B}}$ are omitted. Within this limitation, however, they provide full generality with respect to the tensorial structure of the relationship between $\overline{\boldsymbol{B}}$ and $\overline{\boldsymbol{\mathcal{F}}}$ or $\overline{\boldsymbol{\mathcal{E}}}$. Consequently, it is not necessary to include further terms proportional to the mean flow and its derivatives, as the corresponding coefficients can be covered by the already included ones. For example, to get a contribution of the form $c_{ij}\overline{U}_j$ in the emf we could assume that there is a part of, e.g., $\boldsymbol{\alpha}$ of the form $c_1\overline{U}_i v_j + c_2\overline{U}_j v_i$ with some vector $\boldsymbol{v}$ resulting in $c_{ij} = c_1\boldsymbol{v}\cdot\overline{\boldsymbol{B}}\,\delta_{ij} + c_2\,v_i\overline{B}_j$. The mean velocity plays the role of a "problem parameter" and all transport coefficients can of course be determined as functions of it.

Due to the neglect of the advective term $\boldsymbol{U}\cdot\nabla\boldsymbol{U}$ and the simplification of the viscous term in the model introduced in Sect. 3.1 there is no mean ponderomotive force $\overline{\mathcal{F}}_0$ in the absence of the mean field. However, in proper hydrodynamics, e.g. in the form shown in Appendix A, this quantity shows terms proportional to derivatives of $\overline{\boldsymbol{U}}$. Then, a corresponding test method can be tailored likewise for the coefficients in Eq. (28) which turn into tensors for a general anisotropic background.

Appendix C: Derivation of $\boldsymbol{\phi}(k_z)$, $\boldsymbol{\psi}(k_z)$

Start with the stationary induction equation in SOCA

$$\eta\nabla^2\boldsymbol{b}_{\overline{B}} + \mathrm{curl}\,(\boldsymbol{u}_0\times\overline{\boldsymbol{B}}) = \boldsymbol{0}. \tag{C.1}$$

Assume $\boldsymbol{u}_0 = u_{0\mathrm{rms}}\boldsymbol{f}$ and $\boldsymbol{b}_0 = b_{0\mathrm{rms}}\boldsymbol{f}$ with $\boldsymbol{f} = \boldsymbol{f}(x,y)$, $\mathrm{curl}\,\boldsymbol{f} = k_\mathrm{f}\boldsymbol{f}$, $\overline{\boldsymbol{f}^2} = 1$, $\overline{\boldsymbol{B}} = \hat{\boldsymbol{B}}\mathrm{e}^{\mathrm{i}k_z z}$, and $\hat{B}_{x,y} = \mathrm{const}$, $\hat{B}_z = 0$. Hence $\nabla^2\boldsymbol{f} = -k_\mathrm{f}^2\boldsymbol{f}$. Then we can make the ansatz $\boldsymbol{b}_{\overline{B}} = \hat{\boldsymbol{b}}(x,y)\mathrm{e}^{\mathrm{i}k_z z}$ with $\nabla^2\hat{\boldsymbol{b}} = -k_\mathrm{f}^2\hat{\boldsymbol{b}}$ and get

$$\boldsymbol{b}_{\overline{B}} = \frac{1}{\eta}\frac{1}{k_\mathrm{f}^2+k_z^2}\left[(\overline{\boldsymbol{B}}\cdot\nabla)\boldsymbol{u}_0 - \mathrm{i}k_z\,u_{0z}\overline{\boldsymbol{B}}\right].$$

For the calculation of the mean force

$$\overline{\mathcal{F}}_{\overline{B}} = \overline{\boldsymbol{j}_0\times\boldsymbol{b}_{\overline{B}}} + \overline{\boldsymbol{j}_{\overline{B}}\times\boldsymbol{b}_0}$$

we need further

$$\boldsymbol{j}_{\overline{B}} = \mathrm{curl}\,\boldsymbol{b}_{\overline{B}} = \mathrm{e}^{\mathrm{i}k_z z}(\mathrm{curl}\,\hat{\boldsymbol{b}} + \mathrm{i}k_z\hat{\boldsymbol{z}}\times\hat{\boldsymbol{b}}) \tag{C.2}$$

$$= \frac{k_\mathrm{f}}{\eta(k_\mathrm{f}^2+k_z^2)}\left[(\overline{\boldsymbol{B}}\cdot\nabla)\boldsymbol{u}_0 + \mathrm{i}k_z(\overline{\boldsymbol{B}}\cdot\boldsymbol{u}_0)\hat{\boldsymbol{z}}\right] + \mathrm{i}k_z\hat{\boldsymbol{z}}\times\boldsymbol{b}_{\overline{B}}. \tag{C.3}$$

Consequently,

$$\begin{aligned}\overline{\mathcal{F}}_{\overline{B}} &= k_\mathrm{f}\,\overline{\boldsymbol{b}_0\times\boldsymbol{b}_{\overline{B}}} + \overline{\boldsymbol{j}_{\overline{B}}\times\boldsymbol{b}_0} = \frac{1}{\eta}\frac{1}{k_\mathrm{f}^2+k_z^2}\\ &\quad\left[\mathrm{i}k_z\overline{\left(k_\mathrm{f}(\overline{\boldsymbol{B}}\cdot\boldsymbol{u}_0)\hat{\boldsymbol{z}} + k_\mathrm{f}u_{0z}\overline{\boldsymbol{B}} + \hat{\boldsymbol{z}}\times(\overline{\boldsymbol{B}}\cdot\nabla)\boldsymbol{u}_0\right)\times\boldsymbol{b}_0}\right.\\ &\quad\left. + k_z^2\,\overline{u_{0z}(\hat{\boldsymbol{z}}\times\overline{\boldsymbol{B}})\times\boldsymbol{b}_0}\,\right]\\ &= \frac{1}{\eta}\frac{1}{k_\mathrm{f}^2+k_z^2}\left[\mathrm{i}k_z k_\mathrm{f}\overline{\left((\overline{\boldsymbol{B}}\cdot\boldsymbol{u}_0)\hat{\boldsymbol{z}} + u_{0z}\overline{\boldsymbol{B}}\right)\times\boldsymbol{b}_0}\right.\\ &\quad + \mathrm{i}k_z\overline{b_{0z}(\overline{\boldsymbol{B}}\cdot\nabla)\boldsymbol{u}_0 - \hat{\boldsymbol{z}}\boldsymbol{b}_0\cdot(\overline{\boldsymbol{B}}\cdot\nabla)\boldsymbol{u}_0}\\ &\quad\left. + k_z^2(\overline{u_{0z}b_{0z}}\,\overline{\boldsymbol{B}} - \hat{\boldsymbol{z}}\overline{u_{0z}\boldsymbol{b}_0}\cdot\overline{\boldsymbol{B}})\right]\end{aligned}$$

and with $\overline{\boldsymbol{J}} = \mathrm{i}k_z\hat{\boldsymbol{z}}\times\overline{\boldsymbol{B}}$, that is, $\mathrm{i}k_z B_k = \epsilon_{ki3}\overline{J}_i$, $k=1,2$,

$$\begin{aligned}\overline{\mathcal{F}}_{\overline{B}i} &= \frac{1}{\eta}\frac{1}{k_\mathrm{f}^2+k_z^2}\left[k_\mathrm{f}\left(\epsilon_{i3k}\epsilon_{ml3}\overline{u_{0m}b_{0k}} - \epsilon_{ijk}\epsilon_{kl3}\overline{u_{0z}b_{0j}}\right)\overline{J}_l\right.\\ &\quad+\epsilon_{lj3}\left(-\overline{b_{0z}\frac{\partial u_{0i}}{\partial x_j}} + \delta_{i3}\overline{\boldsymbol{b}_0\cdot\frac{\partial\boldsymbol{u}_0}{\partial x_j}}\right)\overline{J}_l\\ &\quad\left. + k_z^2\left(\overline{u_{0z}b_{0z}}\,\overline{B}_i - \delta_{i3}\overline{u_{0z}b_{0l}}\,\overline{B}_l\right)\right].\end{aligned}$$

The tensors are hence

$$\begin{aligned}\phi_{il} &= \frac{1}{\eta}\frac{k_z^2}{k_\mathrm{f}^2+k_z^2}\left(\overline{u_{0z}b_{0z}}\delta_{il} - \overline{u_{0z}b_{0l}}\delta_{i3}\right),\\ \psi_{il} &= \frac{1}{\eta}\frac{1}{k_\mathrm{f}^2+k_z^2}\left[k_\mathrm{f}(\overline{u_{0z}b_{0z}}\delta_{il} - \overline{u_{0z}b_{0l}}\delta_{i3})\right.\\ &\quad + k_\mathrm{f}(1-\delta_{i3})\left(\overline{u_{0i}b_{0l}} - \delta_{il}(\overline{u_{01}b_{01}} + \overline{u_{02}b_{02}})\right)\\ &\quad\left. + \epsilon_{lj3}\left(\overline{b_{0z}\frac{\partial u_{0i}}{\partial x_j}} - \overline{\boldsymbol{b}_0\cdot\frac{\partial\boldsymbol{u}_0}{\partial x_j}}\delta_{i3}\right)\right],\quad l\neq 3\\ \phi_{i3} &= \psi_{i3} = 0.\end{aligned}$$

For $k_z \ll k_\mathrm{f}$ the tensor $\boldsymbol{\phi}$ is proportional to k_z^2. Thus the corresponding mean force expressed in physical space by a convolution $\check{\boldsymbol{\phi}}\circ\overline{\boldsymbol{B}}$, with $\check{\boldsymbol{\phi}}$ being the Fourier-backtransformed $\boldsymbol{\phi}$, can be approximated by a term $\propto \partial^2\overline{\boldsymbol{B}}/\partial z^2$. For $k_z \gg k_\mathrm{f}$, however, the mean force is represented by a term $\propto \overline{\boldsymbol{B}}$. With Roberts geometry (Eq. (42)) we have for $\sigma = 1$

$$\phi_{11} = \phi_{22} = \frac{1}{2\eta}\frac{k_z^2}{k_z^2+k_\mathrm{f}^2}u_{0\mathrm{rms}}b_{0\mathrm{rms}}\,,\quad \boldsymbol{\psi} = \boldsymbol{0}. \tag{C.4}$$

All other ϕ components vanish, too.

If, however, for the Roberts geometry $0\leq\sigma<1$, the field $\boldsymbol{f}$ has indeed yet the property $\nabla^2\boldsymbol{f} = -k_\mathrm{f}^2\boldsymbol{f}$, but is no longer of Beltrami type. Instead, we have

$$\mathrm{curl}\,\boldsymbol{f} = \sigma k_\mathrm{f}\left[\boldsymbol{f} + \left(\frac{1}{\sigma^2}-1\right)f_z\hat{\boldsymbol{z}}\right].$$

The tensor $\boldsymbol{\psi}$ does not vanish any longer, but is now

$$\begin{aligned}\psi_{11} &= -\frac{1}{\eta(k_z^2+k_\mathrm{f}^2)}\frac{k_y^2(1-\sigma^2)}{k_\mathrm{f}(1+\sigma^2)}u_{0\mathrm{rms}}b_{0\mathrm{rms}},\\ \psi_{22} &= -\frac{1}{\eta(k_z^2+k_\mathrm{f}^2)}\frac{k_x^2(1-\sigma^2)}{k_\mathrm{f}(1+\sigma^2)}u_{0\mathrm{rms}}b_{0\mathrm{rms}},\\ \psi_{12} &= \psi_{21} = 0.\end{aligned}$$

Appendix D: Illustration of extracting a linear evolution equation from a nonlinear one

To illustrate the procedure of extracting a linear evolution equation from a nonlinear problem, let us consider a simple quadratic ordinary differential equation, $y' = y^2$, where a prime denotes here differentiation. We split y into two parts, $y = y_\mathrm{N} + y_\mathrm{L}$, so we have

$$y^2 = y_\mathrm{N}^2 + 2y_\mathrm{N}y_\mathrm{L} + y_\mathrm{L}^2. \tag{D.1}$$

In the last two terms we can replace $y_\mathrm{N} + y_\mathrm{L}$ by y, so we have $2y_\mathrm{N}y_\mathrm{L} + y_\mathrm{L}^2 = (y_\mathrm{N}+y)y_\mathrm{L}$, which is now formally linear in y_L. Here, y corresponds to the solution of the "main run". Consequently, we have

$$\begin{cases} y' = y^2,\\ y_\mathrm{N}' = y_\mathrm{N}^2,\\ y_\mathrm{L}' = (y_\mathrm{N}+y)y_\mathrm{L},\end{cases} \tag{D.2}$$

where the last equation is linear in y_L. Thus, at the expense of having to solve an additional nonlinear auxiliary equation, $y_\mathrm{N}' = y_\mathrm{N}^2$, we have extracted a linear evolution equation for y_L.

Note, that the system (D.2) is exactly equivalent to (D.1), i.e. no approximation has been made.

Appendix E: Derivation of Eq. (45)

Consider the stationary version of (21) with $\mathcal{F}'_{\overline{B}}$ dropped (i.e. SOCA)

$$\nu\nabla^2\boldsymbol{u}_{\overline{B}} + \boldsymbol{j}\times\overline{\boldsymbol{B}} + \overline{\boldsymbol{J}}\times\boldsymbol{b} = \boldsymbol{0}. \tag{E.1}$$

Assume a uniform $\overline{\boldsymbol{B}}$, i.e., $\overline{\boldsymbol{J}} = \boldsymbol{0}$, $\boldsymbol{b} = \operatorname{curl}\boldsymbol{a}$, $\operatorname{div}\boldsymbol{a} = 0$, hence $\boldsymbol{j} = -\nabla^2\boldsymbol{a}$. We get

$$\boldsymbol{u}_{\overline{B}} = \boldsymbol{a}\times\overline{\boldsymbol{B}}/\nu \tag{E.2}$$

and further

$$(\overline{\boldsymbol{u}_{\overline{B}}\times\boldsymbol{b}})_i = \frac{1}{\nu}\epsilon_{ilm}\epsilon_{lkj}\overline{a_k b_m}\,\overline{B}_j = \alpha_{ij}\overline{B}_j$$

that is,

$$\alpha_{ij} = (\overline{\boldsymbol{a}\cdot\boldsymbol{b}}\,\delta_{ij} - \overline{a_i b_j})/\nu.$$

Isotropy results in

$$\alpha = \alpha_{ii}/3 = 2\,\overline{\boldsymbol{a}\cdot\boldsymbol{b}}/3\nu.$$

For $\boldsymbol{b}$ with Roberts geometry (Eq. (42)), however, we have $\alpha = \alpha_{11} = \alpha_{22} \neq \alpha_{33}$, hence

$$\alpha = (\overline{\boldsymbol{a}\cdot\boldsymbol{b}} + \overline{a_3 b_3})/2\nu = k_\mathrm{f}(\overline{\boldsymbol{a}^2} + \overline{a_3^2})/2\nu = 3b_\mathrm{rms}^2/4k_\mathrm{f}\nu$$

and with $\mathrm{Lu} = b_\mathrm{rms}/\eta k_\mathrm{f}$

$$\alpha = \frac{3}{4}\,b_\mathrm{rms}\mathrm{Lu}/\mathrm{Pr}_\mathrm{M}. \tag{E.3}$$

Adopt now $\overline{\boldsymbol{B}}$ depending on z only with $\overline{\boldsymbol{B}} \propto \mathrm{e}^{\mathrm{i}k_z z}$, but $\boldsymbol{a}$ still independent of z. Roberts geometry implies $\nabla^2\boldsymbol{a} = -k_\mathrm{f}^2\boldsymbol{a}$ and $\nabla^2\boldsymbol{u}_{\overline{B}} = -(k_\mathrm{f}^2 + k_z^2)\boldsymbol{u}_{\overline{B}}$. Inserting in (E.1) (with the term $\propto \overline{\boldsymbol{J}}$ omitted) yields

$$\left(k_\mathrm{f}^2 + k_z^2\right)\boldsymbol{u}_{\overline{B}} = k_\mathrm{f}^2\boldsymbol{a}\times\overline{\boldsymbol{B}}/\nu + \ldots$$

and comparison with (E.2) reveals that (E.3) has only to be modified by the factor $1/\left[1 + (k_z/k_\mathrm{f})^2\right]$.

Appendix F: Derivation of α_mk in fourth order approximation

We employ the iterative procedure described, e.g., in Rädler & Rheinhardt (2007) to obtain those contributions to $\overline{\boldsymbol{\mathcal{E}}}_{\overline{B}}$ which are quadratic in $u_{0\mathrm{rms}}$ and $b_{0\mathrm{rms}}$ and expand for that purpose $\boldsymbol{b}_{\overline{B}}$ and $\boldsymbol{u}_{\overline{B}}$ into the series

$$\boldsymbol{b}_{\overline{B}} = \boldsymbol{b}_{\overline{B}}^{(1)} + \boldsymbol{b}_{\overline{B}}^{(2)} + \boldsymbol{b}_{\overline{B}}^{(3)} + \ldots,$$
$$\boldsymbol{u}_{\overline{B}} = \boldsymbol{u}_{\overline{B}}^{(1)} + \boldsymbol{u}_{\overline{B}}^{(2)} + \boldsymbol{u}_{\overline{B}}^{(3)} + \ldots$$

where in the stationary case

$$\eta\nabla^2\boldsymbol{b}_{\overline{B}}^{(1)} = -\operatorname{curl}(\boldsymbol{u}_0\times\overline{\boldsymbol{B}})$$
$$\nu\nabla^2\boldsymbol{u}_{\overline{B}}^{(1)} = -(\boldsymbol{j}_0\times\overline{\boldsymbol{B}} + \overline{\boldsymbol{J}}\times\boldsymbol{b}_0)$$
$$\eta\nabla^2\boldsymbol{b}_{\overline{B}}^{(i)} = -\operatorname{curl}(\boldsymbol{u}_0\times\boldsymbol{b}_{\overline{B}}^{(i-1)} + \boldsymbol{u}_{\overline{B}}^{(i-1)}\times\boldsymbol{b}_0)$$
$$\nu\nabla^2\boldsymbol{u}_{\overline{B}}^{(i)} = -\left(\boldsymbol{j}_0\times\boldsymbol{b}_{\overline{B}}^{(i-1)} + \boldsymbol{j}_{\overline{B}}^{(i-1)}\times\boldsymbol{b}_0\right), \quad i = 2,\ldots$$

and

$$\overline{\boldsymbol{\mathcal{E}}}_{\overline{B}} = \sum_{i=1}^{\infty}\left(\overline{\boldsymbol{u}_0\times\boldsymbol{b}_{\overline{B}}^{(i)}} + \overline{\boldsymbol{u}_{\overline{B}}^{(i)}\times\boldsymbol{b}_0}\right) = \sum_{i=1}^{\infty}\overline{\boldsymbol{\mathcal{E}}}_{\overline{B}}^{(i)}.$$

In the following we assume $\overline{\boldsymbol{B}}$ to be uniform and $\boldsymbol{u}_0$, $\boldsymbol{b}_0$ to have Roberts geometry, see Eq. (42). The SOCA solutions $\boldsymbol{b}_{\overline{B}}^{(1)}$ and $\boldsymbol{u}_{\overline{B}}^{(1)}$ read

$$\boldsymbol{b}_{\overline{B}}^{(1)} = \frac{1}{\eta k_\mathrm{f}^2}(\overline{\boldsymbol{B}}\cdot\nabla)\boldsymbol{u}_0, \quad \boldsymbol{u}_{\overline{B}}^{(1)} = \frac{1}{\nu k_\mathrm{f}}\boldsymbol{b}_0\times\overline{\boldsymbol{B}}.$$

From here on we switch to dimensionless quantities and set $\eta = \nu = 1$, $k_x = k_y = 1$, $k_\mathrm{f} = \sqrt{2}$, $|\overline{\boldsymbol{B}}| = 1$. So we have

$$\boldsymbol{b}_{\overline{B}}^{(1)} = \frac{u_{0\mathrm{rms}}}{2}[\sin x\sin y, \cos x\cos y, -\sqrt{2}\sin x\cos y]$$
$$\boldsymbol{u}_{\overline{B}}^{(1)} = \frac{b_{0\mathrm{rms}}}{2}[0, 2\cos x\cos y, -\sqrt{2}\sin x\cos y]$$
$$\boldsymbol{u}_{\overline{B}}^{(2)} = \boldsymbol{0}$$
$$\boldsymbol{b}_{\overline{B}}^{(2)} = \frac{1}{8}\Bigg(-u_{0\mathrm{rms}}^2[\cos 2y, 0, \sqrt{2}\sin 2y] + \frac{b_{0\mathrm{rms}}^2}{2}$$
$$\times\left[\cos 2y(\cos 2x + 2), \sin 2y\sin 2x, \sqrt{2}\sin 2y(\cos 2x + 3)\right]\Bigg).$$

For $\boldsymbol{b}_{\overline{B}}^{(3)}$ and $\boldsymbol{u}_{\overline{B}}^{(3)}$ we present here only those parts which eventually contribute to α_mk:

$$\boldsymbol{b}_{\overline{B}}^{(3)} = \frac{u_{0\mathrm{rms}}b_{0\mathrm{rms}}^2}{32}[\sin x\sin y, \cos x\cos y, -4\sqrt{2}\sin x\cos y]$$
$$+\ldots$$
$$\boldsymbol{u}_{\overline{B}}^{(3)} = \frac{u_{0\mathrm{rms}}^2 b_{0\mathrm{rms}}}{16}[0, \cos x\cos y, -\frac{\sqrt{2}}{2}\sin x\cos y] + \ldots.$$

Finally,

$$\overline{\boldsymbol{\mathcal{E}}}_{\overline{B}}^{(3)} = \overline{\boldsymbol{u}_0\times\boldsymbol{b}_{\overline{B}}^{(3)}} + \overline{\boldsymbol{u}_{\overline{B}}^{(3)}\times\boldsymbol{b}_0} = -u_{0\mathrm{rms}}^2 b_{0\mathrm{rms}}^2\frac{\sqrt{2}}{64} + \ldots,$$

i.e.

$$\alpha_\mathrm{mk} \approx -u_{0\mathrm{rms}}^2 b_{0\mathrm{rms}}^2\frac{\sqrt{2}}{64}.$$

Note, that the contributions omitted in $\overline{\boldsymbol{\mathcal{E}}}_{\overline{B}}^{(3)}$ provide fourth order corrections to α_k and α_m. They result in dependences on Re_M and Lu that are weaker than the parabolic SOCA ones; see Fig. 3.

References

Beck, R., Poezd, A. D., Shukurov, A., & Sokoloff, D. D. 1994, A&A, 289, 94
Beck, R., Brandenburg, A., Moss, D., Shukurov, A., & Sokoloff, D. 1996, ARA&A, 34, 155
Brandenburg, A. 2001, ApJ, 550, 824
Brandenburg, A. 2005a, ApJ, 625, 539
Brandenburg, A. 2005b, Astron. Nachr., 326, 787
Brandenburg, A., & Käpylä, P. J. 2007, New J. Phys., 9, 305, 1
Brandenburg, A., & Subramanian, K. 2005, Phys. Rep. 417, 1
Brandenburg, A., & von Rekowski, B. 2001, A&A, 379, 1153
Brandenburg, A., Dobler, W., & Subramanian, K. 2002, Astron. Nachr., 323, 99
Brandenburg, A., Rädler, K.-H., & Schrinner, M. 2008a, A&A, 482, 739
Brandenburg, A., Rädler, K.-H., Rheinhardt, M., & Käpylä, P. J. 2008b, ApJ, 676, 740
Brandenburg, A., Rädler, K.-H., Rheinhardt, M., & Subramanian, K. 2008c, ApJ, 687, L49
Brandenburg, A., Kleeorin, N., & Rogachevskii, I. 2010, Astron. Nachr., 331, 5
Cattaneo, F. 1999, ApJ, 515, L39
Cho, J., & Vishniac, E. 2000, ApJ, 538, 217

Courvoisier, A., Hughes, D. W., & Proctor, M. R. E. 2010, Proc. Roy. Soc. Lond., 466, 583
Elperin, T., Golubev, I., Kleeorin, N., & Rogachevskii, I. 2007, Phys. Rev. E, 76, 066310
Emonet, T., & Cattaneo, F. 2001, ApJ, 560, L197
Field, G. B., Blackman, E. G., & Chou H. 1999, ApJ, 513, 638
Frisch, U., She, Z. S., & Sulem, P. L. Phys. D, 198728382
Haugen, N. E. L., Brandenburg, A., & Dobler, W. 2003, ApJ, 597, L141
Haugen, N. E. L., Brandenburg, A., & Dobler, W. 2004, Phys. Rev. E, 70, 016308
Hubbard, A., & Brandenburg, A. 2009, ApJ, 706, 712
Käpylä, P. J., Korpi, M. J., & Brandenburg, A. 2008, A&A, 491, 353
Käpylä, P. J., Mitra, D., & Brandenburg, A. 2009, Phys. Rev. E, 79, 016302
Käpylä, P. J., Korpi, M. J., & Brandenburg, A. 2010, MNRAS, 402, 1458
Kazantsev, A. P. 1968, Sov. Phys. JETP, 26, 1031
Krause, F., & Rädler, K.-H. 1980, Mean-field magnetohydrodynamics and dynamo theory (Oxford: Pergamon Press)
Mitra, D., Käpylä, P. J., Tavakol, R., & Brandenburg, A. 2009, A&A, 495, 1
Moffatt, H. K. 1972, J. Fluid Mech., 53, 385
Moffatt, H. K. 1978, Magnetic field generation in electrically conducting fluids (Cambridge: Cambridge University Press)
Parker, E. N. 1979, Cosmical magnetic fields (Oxford: Clarendon Press)
Pouquet, A., Frisch, U., & Léorat, J. 1976, J. Fluid Mech., 77, 321
Rädler, K.-H., & Brandenburg, A. 2010, Astron. Nachr., 331, 14
Rädler, K.-H., & Rheinhardt, M. 2007, Geophys. Astrophys. Fluid Dyn., 101, 117
Rädler, K.-H., Rheinhardt, M., Apstein, E., & Fuchs, H. 2002a, Magnetohydrodynamics, 38, 41
Rädler, K.-H., Rheinhardt, M., Apstein, E., & Fuchs, H. 2002b, Nonl. Processes Geophys., 38, 171
Rogachevskii, I., & Kleeorin, N. 2000, Phys. Rev. E, 61, 5202
Rogachevskii, I., & Kleeorin, N. 2007, Phys. Rev. E, 76, 056307
Rüdiger, G. 1974, Astron. Nachr., 295, 275
Rüdiger, G. 1980, Geophys. Astrophys. Fluid Dyn., 16, 239
Rüdiger, G. 1982, Geophys. Astrophys. Fluid Dyn., 21, 1
Schekochihin, A. A., Maron, J. L., Cowley, S. C., & McWilliams, J. C. 2002, ApJ, 576, 806
Schekochihin, A. A., Cowley, S. C., Taylor, S. F., Maron, J. L., & McWilliams, J. C. 2004, ApJ, 612, 276
Schrinner, M., Rädler, K.-H., Schmitt, D., Rheinhardt, M., & Christensen, U. 2005, Astron. Nachr., 326, 245
Schrinner, M., Rädler, K.-H., Schmitt, D., Rheinhardt, M., & Christensen, U. R. 2007, Geophys. Astrophys. Fluid Dyn., 101, 81
Solanki, S. K., Inhester, B., & Schüssler, M. 2006, Rep. Prog. Phys., 69, 563
Sulem, P. L., She, Z. S., Scholl, H., & Frisch, U. 1989, J. Fluid Mech., 205, 341
Sur, S., Subramanian, K., & Brandenburg, A. 2007, MNRAS, 376, 1238
Sur, S., Brandenburg, A., & Subramanian, K. 2008, MNRAS, 385, L15
Tilgner, A., & Brandenburg, A. 2008, MNRAS, 391, 1477
Vögler, A., & Schüssler, M. 2007, A&A, 465, L43
Yoshizawa, A. 1990, Phys. Fluids B, 2, 1589